Chelation Equilibria and π-Electron Delocalization in Neutral Hypercoordinate Organosilicon Complexes of Pyrithione

Erin R. Tiede, Matthew T. Heckman, William W. Brennessel,[‡] and Bradley M. Kraft[*†]*

[†] *Department of Chemistry, St. John Fisher University, Rochester, NY 14618, USA*
[‡] *Department of Chemistry, University of Rochester, Rochester, NY 14627, USA*

For Table of Contents Only:

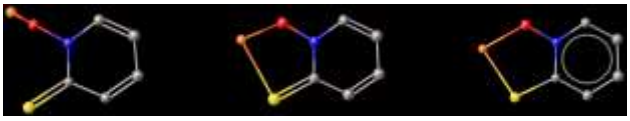

Abstract.

A series of neutral pyrithionato (OPTO) organosilicon compounds, $R_3Si(OPTO)$ (R = Me (**1**), Ph (**2**)), *cis*-$R_2Si(OPTO)_2$ (R = Me (**3**), Et (**4**), ^{i}Pr (**5**), ^{t}Bu (**6**), mesityl (**10**), allyl (**11**), *p*-tolyl (**13**); R_2 = $(CH_2)_3$ (**7**), $(CH_2)_4$ (**8**), $(CH_2)_5$ (**9**), Me, allyl (**12**)), and *cis*-$R_2Si(OPTO)Cl$ (R = Me (**14**), ^{i}Pr (**15**), allyl (**16**), *p*-tolyl (**17**), mesityl (**18**), Ph (**19**)), have been prepared and characterized by ^{1}H, ^{13}C, and ^{29}Si NMR spectroscopy. X-ray crystallographic analysis reveals four-coordinate silicon atoms in **1**, **2**, **6**, and **10**, five-coordinate in **3**, **9**, **11**, **12**, **14-19**, six-coordinate in **7** and **8**, and primarily six-coordinate with co-crystallized five-coordinate forms in **13**. Collectively, a wide range of chelate strengths of the OPTO ligand is observed in these complexes characterized by the Si—S bond length and S—Si—O bite angle in the solid state which correlates well with the solution-state ^{13}C NMR C=S chemical shift. In TBP five-coordinate silicon complexes, the ambidentate potential of the OPTO ligand and π-electron delocalization (π-ED) that occurs within the ligand generally allows the chelate effect to be enhanced with sulfur occupying an equatorial vs. axial position. For **8**, **9**, and **18**, reversible chelation equilibria involving Si←S bond formation and concurrent π-ED has been characterized by variable-temperature ^{13}C and ^{29}Si NMR spectroscopy. Solvents of varying dielectric constant were found to have pronounced effects on the ^{13}C NMR chemical shifts of **1**, **15**, and pyrithione.

Introduction.

The exploration and utility of hypercoordinate organosilicon complexes continues to be an active area of research.[1,2] We are interested in studying the fundamental behavior of families of organosilicon complexes bearing hemilabile chelating ligands that possess one inert and one labile donor.[3] Of particular interest is a subclass of these ligands that become formally aromatic upon forming a chelate

complex, including those of hydroxypyridinone, hydroxypyrone, maltol, tropolone, and their sulfur analogs.[4] The aromatic effects resulting from π-electron delocalization (π-ED) within these ligands and within their formed metallocyclic rings, termed chelatoaromaticity,[5] may contribute to increased stability of their metal complexes and therefore improved utility in biological and medical applications including radiopharmaceuticals,[6] metalloenzyme inhibitors,[7] iron transport,[8] aluminum chelation,[9] diabetes therapy,[10] in the sequestration and separation of rare-earth and heavy metals,[11] among others.[12]

As part of our continuing investigation of the family of organosilicon complexes of 1-hydroxy-2-pyridinone (HOPO),[13] we report here the synthesis, characterization, chelation equilibrium studies, and solvent effects in related pyrithione (HOPTO) complexes.[14,15] The monovalent OPTO ligand can chelate formally through an oxyanion and a dative sulfur linkage or through a thiolate anion and a dative oxo linkage with π-ED occurring (Figure 1). Pyrithione itself has been reported to exhibit solvent-dependent thione/thiol tautomerism,[16] but examples of tunable metal systems that exhibit complete ambidentate flexibility of coordinated OPTO ligands are not known. A survey of transition metal, rare-earth, and main group OPTO complexes in the Cambridge Structural Database (CSD) shows predominantly chelated forms with widely varying extents of π-ED given by their range of pyridine ring and carbon-sulfur bond lengths.[17] Fully π-localized monodentate κ-O metal complexes (**i**) are not known in the literature and only four materials (one Ru complex, one Au complex anion, two Os complexes, and one Cd-based coordination polymer) with fully delocalized monodentate κ-S bonding modes (**iv**) are known.[18,19]

Figure 1. Unchelated and chelated forms of the OPTO ligand.

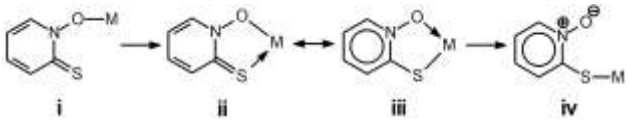

In the present work, we report a family of tri- and diorganosilicon complexes that provide structural and spectroscopic snapshots of the varying levels of chelation and π-ED that occur along the **i**→**ii**→**iii** continuum. The first examples of monodentate κ-O OPTO ligands with fully π-localized systems have been structurally characterized and signature changes in the ^{13}C NMR spectra representing the κ-O/κ-O,S chelation equilibrium and π-ED have been identified. Across the continuum between resonance structures **ii** and **iii**, chelate strength is found to increase *in tandem* with π-ED within the limit of M—S covalent bond formation. Throughout this work, we use the carbon labeling scheme in Figure 2 for the canonical electronic structures of κ-O unchelated and chelated forms.

Figure 2. Labeling scheme for general electronic structures of localized unchelated and delocalized chelated complexes.

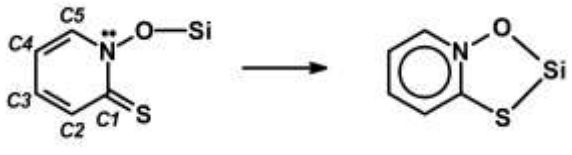

Results and Discussion.

R_3Si(OPTO) Complexes. Triorganosilicon complexes, R_3Si(OPTO) (R = Me (**1**), Ph (**2**)), were prepared in near quantitative yield by reaction of pyrithione, triethylamine, and the corresponding silyl chloride in THF (eq 1). Filtration and removal of the solvent afforded **1** and **2** as yellow powders. These and all other complexes described in this work were found to be generally sensitive to heat and light, decomposing to form a mixture of unidentified products.[20] Pyrithione and related carbon-based thiohydroxamic esters are well known to undergo photochemical processes involving N—O bond cleavage.[21]

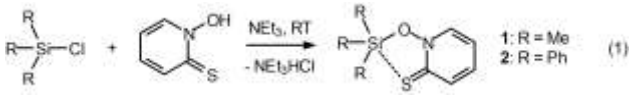

The X-ray crystal structures of **1** and **2** are shown in Figure 3. Selected bond distances and angles are given in Table S5. Both structures exhibit pseudotetrahedral coordination spheres and form a covalent bond between silicon and the hydroxylamine oxygen as is also observed in their 1-oxo-2-pyridinone (OPO) analogs.[13] This bonding arrangement contrasts with most known structures of simple hydrocarbon-based OPTO derivatives which are *N*-oxides with covalent C-S-C linkages,[22] although one thione derivative structure has been reported.[23] In the pentylation of OPTO salts, both *O*- and *S*-alkylated products are formed with product distributions highly dependent on solvent and choice of cation.[24] In our work, silylation of oxygen was observed exclusively.[25]

Figure 3. Thermal ellipsoid plots of **1** and **2** at the 50% probability level with hydrogen atoms omitted.

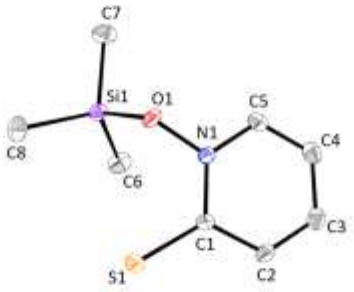

1

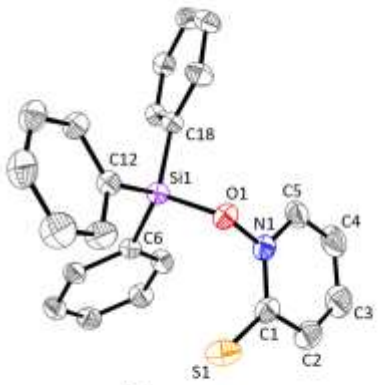

2

The π systems of **1** and **2** are largely localized as given by the sequence of longer C1-C2 and C3-C4 bonds and shorter C2-C3 and C4-C5 bonds similar to those in the free protonated ligand.[24,26] Weak Si←S dative interactions in **1** and **2** are indicated by the long Si···S internuclear distances that are slightly less than the sum of the Si and S van der Waals radii of 3.90 Å.[27] The chelate interaction in **2** is slightly weaker than that in **1** given by the longer Si···S distance (3.8515(6) vs. 3.6016(7) Å), and by the slightly shorter C=S bond lengths (1.674(1) vs. 1.681(1) Å) and C2-C3 (1.359(2) vs. 1.371(2) Å) which point to less π-ED occurring in the pyridine ring.[28] The C=S bond lengths in **1** and **2** are comparable to that in the free ligand (1.684(2) Å) of which is elongated due to an intramolecular non-classical H-bonding interaction between the hydroxyl group and sulfur atom.[26] The opposite effect of ancillary ligands is observed in the related $R_3Si(OPO)$ complexes where a stronger dative Si←OC interaction was observed in $Ph_3Si(OPO)$ vs. $Me_3Si(OPO)$ in both the solid and solution states.[13a] Future computational studies, specifically an energy decomposition analysis, might offer an explanation.

Predominantly 4-coordinate silicon in **1** and **2** is observed in $CDCl_3$ solution ($\delta(^{29}Si)$ = +39.8 and +2.5 ppm, respectively).[29] This is further indicated by the ^{13}C NMR C=S signals of **1** and **2** appearing significantly downfield (δ 175.5 and 176.0 ppm, respectively) similar to that of the hydroxamic acid methyl ester (δ 175.5 ppm) where chelate interactions that would lengthen the C=S bond are absent.[24]

$R_2Si(OPTO)_2$ Complexes. Diorganosilicon complexes, $R_2Si(OPTO)_2$ (R = Me (**3**), Et (**4**), ^{i}Pr (**5**), mesityl (**10**), allyl (**11**), Me, allyl (**12**) and R_2 = $(CH_2)_3$ (**7**), $(CH_2)_4$ (**8**), $(CH_2)_5$ (**9**)), were prepared similarly according to eq 2. For the synthesis of ^{t}Bu$_2$Si(OPTO)$_2$ (**6**), a stronger base, 1,8-diazabicyclo[5.4.0]undec-7-ene (DBU), was required (eq 3). The reaction to form **6** with NEt_3 at 60 °C

after 1 day was incomplete and points to a kinetically slower ligand substitution reaction than with DBU. Trans-silylation of $^{t}Bu_2SiCl_2$ and 2 equiv. **1** at room temperature in an NMR tube reaction in $CDCl_3$ produced no observable **6** in solution.

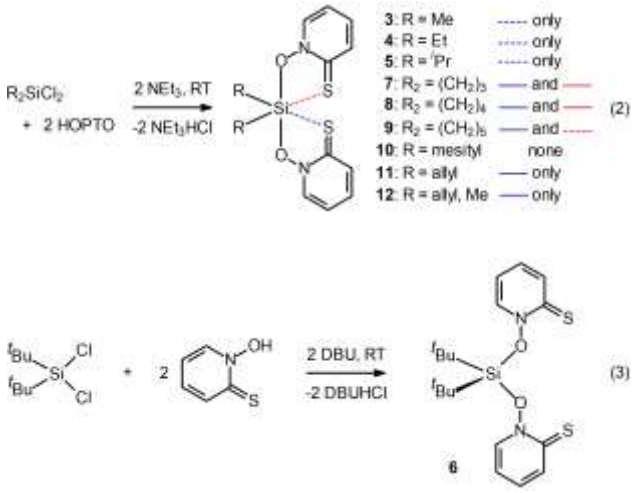

The X-ray crystal structure of **3** reveals 5-coordinate silicon in a distorted trigonal bipyramidal geometry with one monodentate and one weakly chelated OPTO ligand (Figure 4). Selected bond distances and angles are given in Table S6. The chelate interaction in an axial position is characterized as weak by the long Si–S distance (d = 2.5732(8) Å) and by the identical C=S bond lengths of both chelated and unchelated ligands (1.687(2) and 1.686(2) Å, respectively). These bond lengths are comparable to those in unchelated complexes **1** and **2** and point to very little π-ED occurring in either ligand.[30]

Figure 4. Thermal ellipsoid plots of **3**, **6**, **7**, **8**, **9**, **10**, **11**, **12**, and **13** at the 50% probability level with hydrogen atoms omitted. For **7**, **12**, and **13**, only the major component of disorder is shown. For **8** and **11** only one of the two independent molecules is shown.

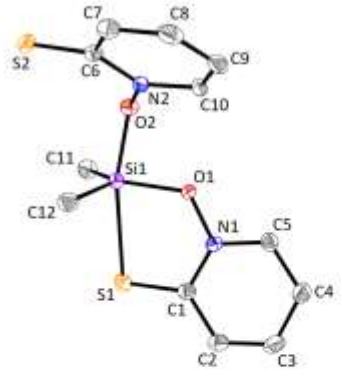

3

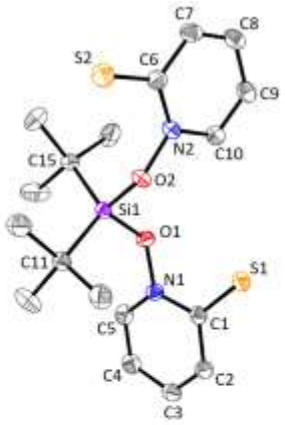

6

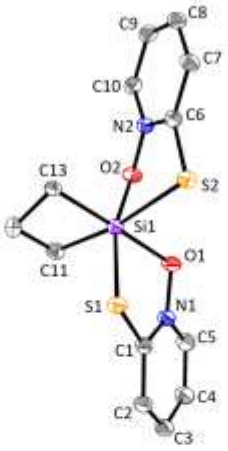

7

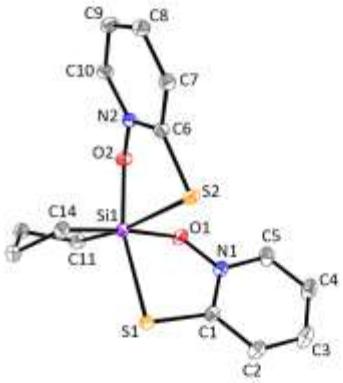

8

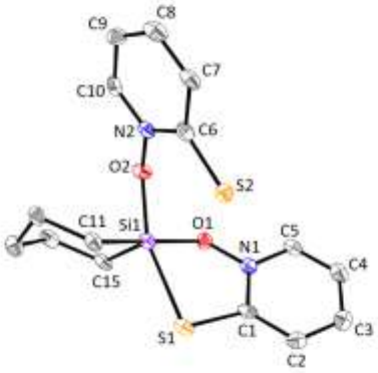

9

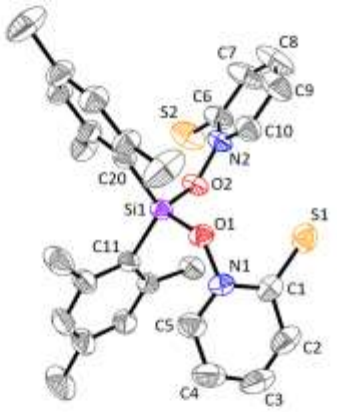

10

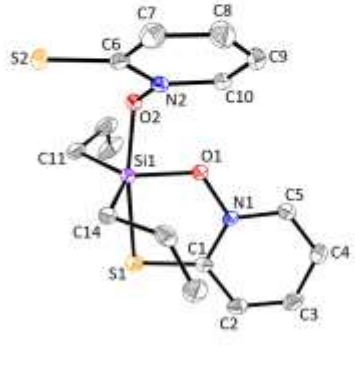

11

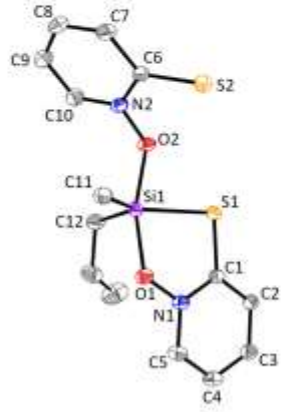

12

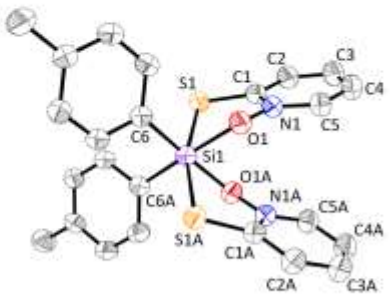

13

The X-ray crystal structure of **6** exhibits 4-coordinate silicon in a tetrahedral geometry with effectively two monodentate OPTO ligands ($d_{Si...S}$ = 3.805, 4.169 Å) (Figure 4). Selected bond distances and angles are given in Table S6. Intermolecular π-stacking is observed between pyridine rings N2, C6-C10 (~3.4-3.5 Å) and may have contributed to the tendency of **6** to crystallize in comparison with **4** and **5** which were isolated as viscous oils at room temperature.

^{13}C NMR studies in $CDCl_3$ indicate that dialkylated complexes **3-5** have similar chelate interactions as given by their similar C=S chemical shifts (δ 170.1, 170.3, and 169.8 ppm, respectively). These upfield shifts relative to those in **1** and **2** are consistent with increased 5-coordinate character in **3-5** in solution as they indicate greater thiol character of the carbon-sulfur bonds as a result of π-ED within the ligand.[24] Interestingly, the ^{29}Si NMR chemical shifts of **3-5** (δ −19.0, −20.2, and −28.4 ppm, respectively) trend toward higher field as the sterics of the alkyl groups increase but this does not support a gradual increase in chelate strength. In $CDCl_3$, the ^{29}Si NMR chemical shifts of independently prepared $Me_2Si(OPh)_2$, $Et_2Si(OPh)_2$, and $^{i}Pr_2Si(OPh)_2$ (Ph = phenyl), which necessarily possess 4-coordinate silicon, trend similarly upfield (δ −5.5, −7.0, and −12.7 ppm, respectively). These observations demonstrate that the ^{29}Si NMR chemical shift as a metric for assessing chelate strength can be confounded by simple ancillary ligand effects and that the ^{13}C NMR C=S chemical shift serves as a more reliable metric. Increasing sterics further in **6**, the ^{29}Si NMR chemical shift (δ −2.6 ppm) and low field ^{13}C NMR C=S signal (δ 174.6 ppm) are consistent with tetracoordinate silicon and unchelated OPTO ligands. In our earlier work with related hexacoordinated $R_2Si(OPO)_2$ complexes, increased R-group sterics promoted dechelation by Si←O=C bond dissociation.[13a] By contrast, owing to their lower coordination number, increasing sterics in these $R_2Si(OPTO)_2$ complexes from R = Me→Et→^{i}Pr has little or no observable effect on chelation until R = ^{t}Bu.

In $CDCl_3$ solution, complexes **3-5** exhibit a single set of five ^{13}C NMR signals for both chelated and unchelated OPTO ligands and indicates a rapid equilibrium between chelated and unchelated states and/or a degenerate windscreen wiper exchange process in which the uncoordinated thione group displaces the coordinated thione group.[3,31] A VT-NMR experiment of **5** in $CDCl_3$ shows small downfield shifts of the ^{13}C and ^{29}Si resonances with increasing temperature indicative of an average increase in Si←S bond dissociation.[32] The remaining four ^{13}C resonances also shift in directions indicative of a decrease in π-ED (vide infra).

Silacycloalkane Complexes. A series of silacycloalkane complexes was synthesized to examine the dependence of silacycles and their ring size on chelation of the OPTO ligand. The silacyclobutane (**7**), –pentane (**8**), and –hexane (**9**) complexes exhibit markedly different ^{29}Si NMR chemical shifts at room

temperature in $CDCl_3$ (δ −111.7, −80.2, and −32.9 ppm, respectively) and indicates that chelation is increasingly favored as the number of carbons in the silacycle decreases.[33] A comparison of the ^{13}C NMR C=S chemical shifts of **7-9** (δ 162.7, 163.4, and 169.2 ppm, respectively) with open-chain complexes **3-5** (all δ ~170 ppm) indicates a stronger chelate effect in the silacycles in particular for **7** and **8**.
In their crystal structures, complexes **7** and **8** feature distorted octahedral coordination spheres with bischelated OPTO ligands and as single isomers having all-*cis* arrangements (Figure 4). Selected bond distances and angles are given in Tables S6-S7. On the basis of Si-O and Si-S bond lengths alone, the chelate interactions in **7** and **8** appear effectively the same, but the larger O-Si-S bite angles in **7** (S1-Si1-O1, 82.86(3)° and S2-Si1-O2, 82.57(3)°; avg. 82.72(4)°) vs. those in **8** (S1-Si1-O1, 82.24(4)°, S2-Si1-O2, 82.20(5)°, S3-Si2-O3, 81.97(4)°, and S4-Si2-O4, 80.99(4)°; avg. 81.85(9)°) indicate an overall closer approach of the ligand to the metal and suggests stronger chelate interactions in **7**. This difference is attributed to the reduced steric demand on the silacyclobutane complex[34] given by its smaller C-Si-C angle [77.42(15)° in **7** vs. 93.23(8)° in **8**] and to the phenomenon of ring-strain enhanced Lewis acidity.[35] Compared with the structure of $(CH_2)_3SiCl_2$, the C-Si-C angle in **7** contracts (Δ = 5.1°) upon complexation of the OPTO ligands apparently due to steric requirements of the OPTO ligands.[36] Despite this contraction, this reflects a net relief in ring strain as a result of the $T_d \rightarrow O_h$ shape transformation that occurs upon chelation.[37] The Si—S bond lengths in both **7** and **8** are ~0.1 Å longer than the average Si—S bond length (2.28 Å) in hexacoordinated phenylthiolate complexes according to the Cambridge Structural Database (CSD)[17] and suggests the limits of Si—S covalent bond formation and π-ED have not been reached in these complexes.

The molecular structure of **9** adopts a primarily square pyramidal geometry[38] with one fully chelated and one weakly chelated OPTO ligand with its sulfur atom located off the vacant coordination site (Figure 4). Selected bond distances and angles are given in Table S7. In comparison with the open-chain complex **3**, shorter Si···S internuclear distances are observed in both its chelated (2.3318(19) Å in **9**; 2.5731(7) Å in **3**) and weakly chelated/unchelated (2.7053(19) Å in **9**; 3.9556(8) Å in **3**) ligands. Lacking significant ring strain in **9**, the stronger chelate effect in **9** may be explained by its reduced steric demand given by its smaller C-Si-C angle (99.6(2)° in **9**; 120.62(10)° in **3**), and by its larger R substituent resulting in an increased electron-withdrawing effect. These observations are consistent with the slightly higher field ^{29}Si NMR and ^{13}C NMR C=S signals of **9** vs. **3** in solution.

Diarylated Complexes. $(Mesityl)_2Si(OPTO)_2$ (**10**) was prepared according to the methodology of eq 2. The X-ray structure of **10** shows 4-coordinate silicon in a tetrahedral geometry (Figure 4). The large

internuclear separation of silicon and sulfur atoms (d = 3.8790(8) Å and 4.3497(8) Å) and short C=S bond lengths (1.670(2) and 1.673(2) Å) indicate virtually no chelate interaction occurring.

Contrary to expectations, the synthesis of the less sterically-encumbered diarylated complex, (p-tolyl)$_2$Si(OPTO)$_2$ (**13**), proved more difficult. The reaction of (p-tolyl)$_2$SiCl$_2$ with 2 equiv. HOPTO and 2 equiv. NEt$_3$ in THF produced a mixture of **13** and (p-tolyl)$_2$Si(OPTO)Cl, **17**. Trans-silylation of (p-tolyl)$_2$SiCl$_2$ with 2 equiv. of **1** in CDCl$_3$ also produced a mixture of **13**, **17**, Me$_3$SiCl, unreacted **1**, and unidentified products. Although the proportion of **13** was increased significantly in the reaction by subjecting the trans-silylation mixture to three consecutive evaporation/reconstitution cycles to remove the volatile Me$_3$SiCl byproduct and shift the equilibrium toward product (eq 4), efforts to isolate an analytically pure sample of **13** were unsuccessful although it was possible to isolate single crystals suitable for X-ray crystal structure analysis.[39]

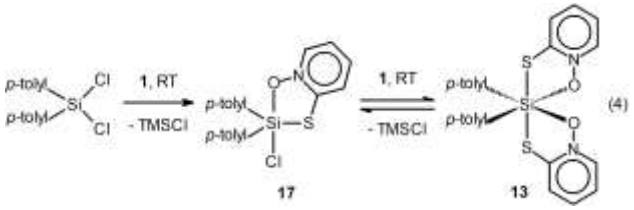

The X-ray structure of **13** shows primarily (92.3%) 6-coordinate silicon in a distorted octahedral geometry with *cis*-aryl groups (Figure 4). Disorder modeling indicates two additional monodentate modes (7.7%) in the structure. Selected bond distances and angles are given in Table S8. In CDCl$_3$ solution, pentacoordinate silicon is indicated by ^{29}Si NMR (δ −70.1 ppm). The lower coordination number in solution together with the presence of co-crystallized monodentate modes indicates a small energy difference between chelated and unchelated forms.

By comparison of **3** and **13**, the more electron-withdrawing p-tolyl vs. Me group imparts a stronger chelate effect in solution given by its higher field ^{13}C C=S chemical shift (δ 166 vs. 170 ppm). In the solid state, a higher coordination number is observed in addition to shorter Si—S (2.3517(6) Å in **13** vs. 2.5731(7) Å in **3**) and longer carbon-sulfur bonds (1.710(3) Å in **13** vs. 1.687(2) Å in **3**). This difference in chelate effect is surprising in light of the greater difficulty of chloride ligand substitution in the synthesis of **13** vs. **3**.

R$_2$Si(OPTO)$_2$ (R$_2$ = Me$_2$, Me(allyl), allyl$_2$) Complexes. For the series of pentacoordinate silicon complexes, R$_2$Si(OPTO)$_2$ (R$_2$ = Me$_2$ (**3**), Me(allyl) (**12**), allyl$_2$ (**11**)), the upfield progression in both ^{29}Si NMR (δ −19.0, −35.3, and −49.0 ppm, respectively) and ^{13}C NMR C=S signals (δ 170.1, 167.5, and 167.1 ppm, respectively) in CDCl$_3$ support that allyl groups increase the Lewis acidity of silicon in comparison

to methyl groups leading to a stronger chelate interaction. In the solid state, an anomaly of this trend is observed with the mixed derivative **12** exhibiting the strongest chelate effect given by its largest S1-Si1-O1 bite angle (84.83(3)°), longest carbon-sulfur bond (d = 1.7275(12) Å), and shortest Si—S bond (d = 2.2057(5) Å). This anomaly may be explained by the difference in the orientation of chelated OPTO ligand with the structure of **12** favoring the S_{eq} arrangement and with the structures of **3** and **11** favoring the S_{ax} arrangement (Figure 4). In line with the discussion below with $R_2Si(OPTO)Cl$ complexes, this observation supports an increased chelate effect when sulfur occupies an equatorial position. The regular expected spectral trends in solution and variation in S_{ax}/S_{eq} orientations in the solid state suggest that energy differences between these isomers are small and are easily influenced by solvation and/or crystal packing effects.

$R_2Si(OPTO)Cl$ Complexes. Monosubstituted complexes of the form $R_2Si(OPTO)Cl$ (R = Me (**14**), ^{i}Pr (**15**), allyl (**16**), *p*-tolyl (**17**), mesityl (**18**)) were prepared according to eq 5. Complex **14** was characterized in solution by NMR spectroscopy only and could not be isolated as a pure solid. Recrystallization of the product residue of **14** resulted in isolation of analytically pure **3** due to ligand redistribution. $Ph_2Si(OPTO)Cl$ (**19**) was synthesized by trans-silylation of Ph_2SiCl_2 with 1 equiv. of **1** (eq 6).

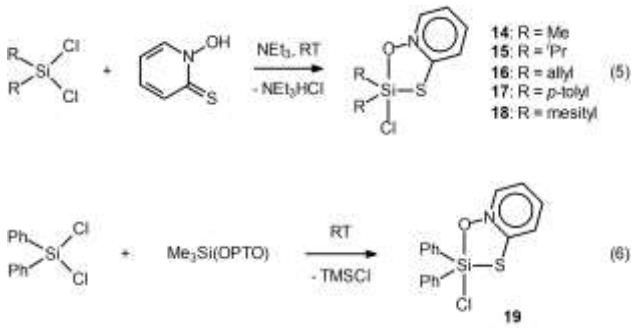

The X-ray crystal structures of **15-19** are given in Figure 5. Selected bond distances and angles are given in Tables S9-S10. All of the compounds exhibit similar distorted trigonal bipyramidal geometries with *cis* carbon-based groups, chloride in axial positions,[40] and chelated OPTO ligands with sulfur in equatorial positions. Compared with all other complexes in this work, these $R_2Si(OPTO)Cl$ complexes possess the strongest chelate interactions given by their longest carbon-sulfur bonds (range = 1.723-1.733 Å), largest O1-Si1-S1 bite angles (range = 85.3-87.5°), and most pronounced extent of π-ED within the pyridine rings (vide infra). A comparison with fully delocalized 2,2'-dithiobis(pyridine-*N*-oxide) (**20**), having longer C—S bond lengths of ~1.76 Å (see the Supporting Information), suggests that maximum π-ED has not been realized in the $R_2Si(OPTO)Cl$ complexes and supports their electronic structures to be between those of **ii** and **iii** (Figure 1). Further, the N-O bond lengths are decreased upon chelation

(1.382(2) Å in **1** vs. 1.3433(10) Å in **15**) but are considerably longer than that in pyridine *N*-oxide (1.314(6) Å).[41] This supports electronic structures of **15-19** closer to **iii** than towards the monodentate κ-S form **iv** (Figure 1) as the negative charge of the bidentate OPTO ligand cannot be localized entirely on the oxygen atom. Variations of ancillary ligand sterics and electronics of **15-19** show little effect on the carbon-sulfur bond lengths although an increase in chelate strength with more electron-withdrawing aryl groups in **17** and **19** vs. **15** is given by the slightly shorter Si-O and Si-S bond lengthss and larger bite angles.

Figure 5. Thermal ellipsoid plots of **15-19** at the 50% probability level with hydrogen atoms omitted. For **16**, only the major component of disorder is shown.

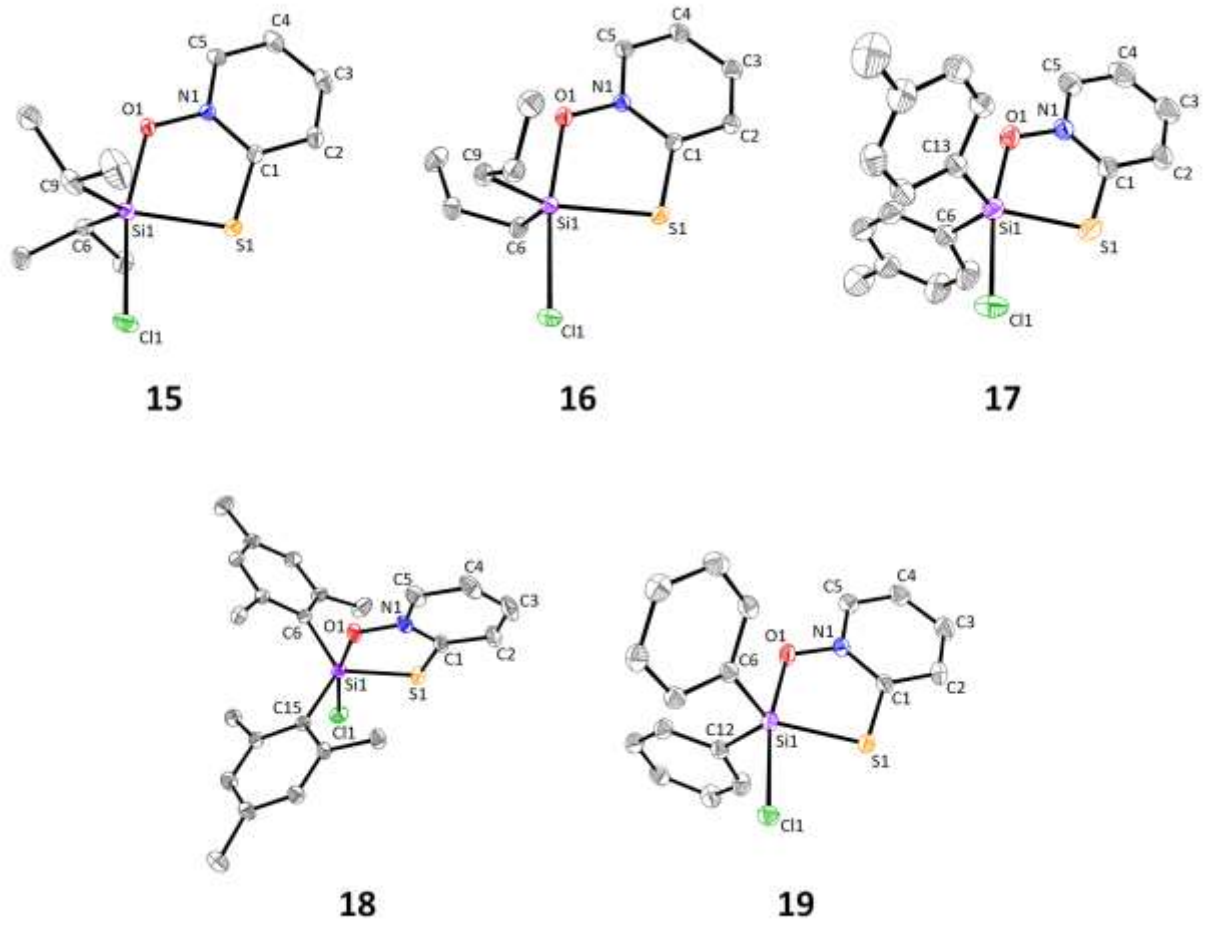

The markedly stronger chelate effect observed collectively in the $R_2Si(OPTO)Cl$ complexes may be explained by the electronic versatility of the OPTO ligand in forming primarily covalent bonds to

silicon with either S or O and the greater tendency for its sulfur atom to occupy an equatorial position. With two possible orientations of the OPTO ligand, S-equatorial (S_{eq}) and S-axial (S_{ax}), the S_{eq} arrangement is expected to increase the covalent character of the Si—S bond in accord with the concept of equatoriphilicity as described for pentacoordinate phosphorus complexes that indicates increased stability with formally anionic donors in the equatorial plane.[42] The more stable S_{eq} bonding arrangement is also consistent with fundamental tendencies for larger and less electronegative atoms to occupy equatorial sites in TBP complexes.[43] In further support of this effect here, the Si—S bond distances in **15-19** (range = 2.18-2.21 Å) are shorter or comparable to the average Si—S covalent bond distance in pentacoordinated phenylthiolate complexes (2.23 Å) according to the CSD.[17] With the ambidentate potential of the OPTO ligand and primarily covalent character of the Si—S bond in an equatorial position, the accessibility of resonance structure **iii** is increased (Figure 1) by which π-ED in the pyridine ring can stabilize the complex to a greater extent than with an Si-S bond in an axial position. Furthermore, axial Si—O bonds are expected fundamentally to become longer and more dative in character due to a greater number of destabilizing 90° bond pair interactions. The Si—O bonds in **15-19** (range = 1.84-1.88 Å) can be characterized as dative. Although there are no known published structures of pentacoordinated organosilicon complexes that contain well-defined dative *N*-oxides, we have synthesized recently one such complex of 8-oxoquinoline *N*-oxide (QNO), $Et_2Si(QNO)Cl$. In this complex, a covalent Si—O bond is formed in an equatorial position with an Si←ON dative interaction in an axial position with its length (d = 1.8684(12) Å) comparable with those in **15-19**.[44] The same S_{eq} arrangement is favored in the stannane congeners, $R_2Sn(OPTO)Cl$ (R = Me, Ph).[45]

In contrast, the S_{ax} arrangements observed in $R_2Si(OPTO)_2$ complexes **3** and **11** indicate stronger covalent Si—O bonds in the equatorial plane and a resonance structure closer to **ii** than **iii** (Figure 1). In the S_{ax} conformation, the naturally longer Si—S internuclear distance in an axial position reduces the extent by which π-ED can occur as observed. The tendency to favor S_{ax} over S_{eq} arrangements in these cases is possibly due to the well-known propensity of silicon to form particularly strong Si—O covalent bonds which is enhanced in an equatorial position, and in these cases, outweighs the stabilization due to π-ED.

The ^{13}C NMR C=S signals (range = δ 154-156 ppm) of **15-17** and **19** in $CDCl_3$ are in agreement with their S_{eq} orientations and strong chelate interactions observed in their solid states. For **18**, its intermediate C=S ^{13}C NMR chemical shift of δ 163.3 ppm suggests that this complex is particularly better solvated and leads to weaker chelation in solution.[46]

Structural Characterization of π-ED. The use of a tunable silicon core as a chelating center has afforded the crystallographic characterization of complexes with widely varying degrees of stabilizing π-

ED occurring within the pyridine ring. Upon chelation, equalization of C-C bond lengths is expected in progressing from a localized to a delocalized aromatic π-system with lengthening of the C=S, C2-C3, and C4-C5 bonds and shortening of the C1-N, C1-C2, C3-C4, and C5-N bonds (Figure 2). These changes are fully consistent with the differences observed in the pyridine ring bond lengths of the strongly chelated monosubstituted $R_2Si(OPTO)Cl$ (**15-19**) complexes in comparison with unchelated $R_3Si(OPTO)$ (**1** and **2**) complexes (Tables S5,S9, and S10). Specifically, in comparison of monosubstituted unchelated **2** with strongly chelated **19**, the C=S, C2-C3 and C4-C5 bonds are longer in **19** (Bond length difference (Δ) = 0.059(2), 0.022(4), and 0.013(4) Å, respectively), and the C1-N, C1-C2, C3-C4, and C5-N bonds are shorter (Δ = 0.034(3), 0.029(4), 0.023(4), and 0.014(3) Å, respectively). In comparison of disubstituted bis-unchelated **6** with strongly bis-chelated **7**, the same trends are observed, but to a lesser extent with the C=S, C2-C3, and C4-C5 bonds longer (Δ = 0.0288(26), 0.016(4), and 0.011(4) Å, respectively), and the C1-N, C1-C2, C3-C4, and C5-N bonds shorter (Δ = 0.013(3), 0.020(4), 0.011(4), and 0.007(3) Å, respectively) in **7**. The lesser extent by which π-ED occurs in 6- vs. 5-coordinate silicon complexes may be due to increased electron density on silicon which decreases the extent by which the C=S bond is able to delocalize toward formation of anSi—S bond, although DFT calculations are needed for an understanding of the charge distribution in these molecules. For **11** and **12**, the same differences in bond lengths are observed in comparing the κ^2- and κ^1-OPTO ligands within each complex (Table S8). For very weakly chelated ligands in **3** and **9**, a smaller extent of pyridine ring bond length differences is observed in comparison with that in unchelated **2**. These general patterns and snapshots of a variety of complexes demonstrate that π-ED within the OPTO ligand occurs in tandem with chelation.

In **1-3**, **6**, and **10-12**, the plane of the monodentate OPTO ligands generally sits orthogonal (range = 80.59-89.11°) to the plane formed by the Si, O, and N atoms. This arrangement minimizes repulsions between the lone pairs on oxygen and the π-localized lone pair on nitrogen.[47] In the most strongly chelated complexes **15**, **17-19**, with the nitrogen lone pair delocalized, the OPTO ligand becomes essentially coplanar with its chelate ring forming small dihedral angles (range = 2.08 – 8.18°; defined as the angle between the S1-Si1-O1 and S1-C1-C2-C3-C4-C5-N1-O1 planes). For **16**, a larger dihedral angle is observed (19.34(2)°). Weak π-stacking of pyridine rings occurs in both **15** and **16** with centroid-centroid distances of 3.7 Å and 4.4 Å, respectively.

The extent of π-ED in the OPTO ligand given by the elongation of the C=S bond can be traced to more direct indicators of chelate strength, specifically the Si—S bond length and the S—Si—O bite angle. Upon examination of the chelated ligands in all complexes in this work, the S—Si—O bite angle is found to correlate directly with the carbon-sulfur bond distance (Figure S2) and the Si—S internuclear distance is found to correlate inversely with the carbon-sulfur bond distance (Figure S3). These regular

trends support that the extent of π-ED correlates with chelate strength. Furthermore, the *average* carbon-sulfur bond distances within individual chelated, unchelated, and mixed κ_1/κ_2 complexes correlate notably well with their respective ^{13}C NMR C=S chemical shift (Figure 6) and supports (1) the agreement of chelate strength indicators between solution-state and solid-state structures, (2) that solvent effects on chelate strength are consistent and small in $CDCl_3$, and (3) that chelation and π-ED within the OPTO ligand occur in tandem along a continuum.

Figure 6. Plot of the ^{13}C NMR C=S chemical shifts at 296 K of **1-3**, **6-13**, and **15-19** in $CDCl_3$ vs. carbon-sulfur bond distance in the solid state. For disubstituted complexes, the average of the carbon-sulfur distances was used. Linearized equation: $y = -334x + 752$. $R^2 = 0.888$.

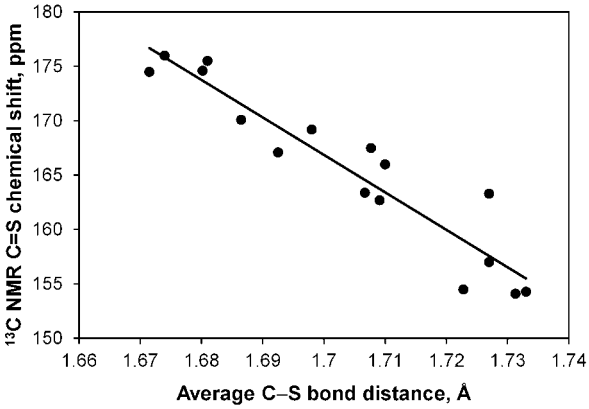

For unknown reasons, a significant narrowing of the NCS angle was found to occur upon π-ED in general with values consistently in the range of ~122-123° in κ^1 form and ~115-117° in κ^2 form across all complexes in this work (Tables S5-S10) However, narrowing of this angle is observed to occur even without complexation with silicon as evidenced in the fully delocalized structure of **20** (Figure S1). In comparison, the CNO angle is much less flexible and ranges from ~118–120° in all complexes and in **20**.

Comparative ^{13}C NMR Analysis. The ^{13}C NMR spectra of complexes **1**, **8**, **9**, and **15**, arranged in order of chelate strength, is given in Figure 7.[48] Carbon resonances of the OPTO ligand in each complex were assigned with ^{1}H-^{13}C HMQC NMR experiments. Carbons **a**, **b**, and **e** appear farther upfield and carbons **c** and **d** appear farther downfield as chelate strength increases and results in a variation in the relative ordering of resonances **b**, **c**, and **e** in **1**.

Figure 7. Zoomed ^{13}C NMR spectra of **1**, **8**, **9**, and **15** in $CDCl_3$ at room temperature in order of increasing chelate strength.

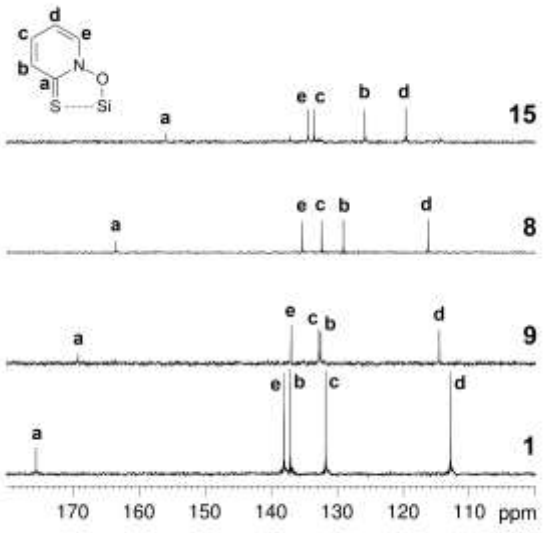

With **1** and **15** serving as prototypes for extremes of unchelated and chelated forms, the X-ray structure data can explain both the direction and extent of shifting of the solution-state pyridine ring ^{13}C NMR signals. By calculating the difference in the average of the two C—X (X=C, N) internuclear distances to each pyridine ring atom, carbons **a** and **b** were found to be closer in **15** than in **1** by 0.024(3) Å and 0.011(3) Å, respectively (Table S11) and points to an overall increase in local π-bonding. Likewise, by ^{13}C NMR spectroscopy, carbons **a** and **b** are observed to shift to the greatest extent and appear upfield by 19.5 ppm and 11.3 ppm in **15** vs. **1**, respectively, as would be expected from a proportional increase in shielding of these carbon atoms from an overall increase in π-bonding. The ^{13}C NMR shift differences for carbons **c**, **d**, and **e** in **15** vs. **1** are much smaller as chelate strength varies and likewise the differences in average internuclear distances between these atoms were expectedly small such that to within their standard uncertainties could not be reliably correlated with the ^{13}C NMR chemical shifts.

Dynamic Chelation Equilibria. A VT-NMR study of **9** in toluene-d_8 revealed a downfield shift of its ^{29}Si NMR signal from δ −73.3 to −55.4 ppm with increasing temperature from −90 to 24 °C in addition to temperature-dependent chemical shifts of the five ^{13}C OPTO ligand resonances (Figure 8). As the temperature is increased and the extent of chelation decreases, carbon resonances **a**, **b**, and **e** shift downfield and resonances **c** and **d** shift upfield with carbon **a** shifting to the largest extent. These

observations are consistent with a dynamic equilibrium between 5- and 4-coordinate states occurring by Si←S bond dissociation (eq 7).[49]

Figure 8. Plot of the ^{13}C NMR spectra of **9** vs. temperature in toluene-d_8. Resonances **b** and **c** cross each other at 34 °C.

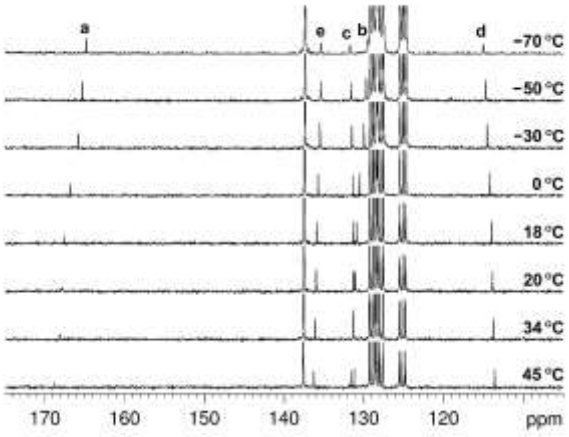

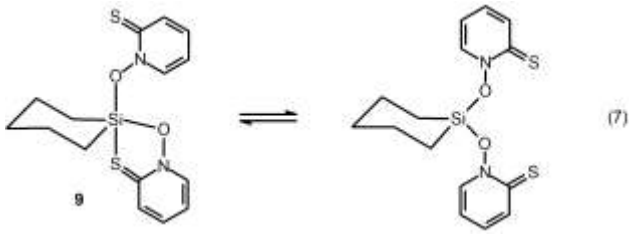

The hexacoordinate silicon complexes **7** and **8** exhibited the same pattern of shifts with temperature but to a lesser degree than that of **9**.[50] These observations point to increased chelate strength in **7** and **8** vs. **9**, consistent with increased Lewis acidity in the smaller silacycles. In **8**, a small solvent-dependence on the ^{29}Si NMR chemical shift at room temperature was observed (δ −80.2 ppm in $CDCl_3$; −86.3 ppm in toluene-d_8) and exhibited a greater rate of downfield shift of the ^{29}Si NMR signal with increasing temperature in $CDCl_3$ (0.096 ppm/K) vs. toluene-d_8 (0.067 ppm/K).[51]

VT-NMR studies of the more strongly chelated $R_2Si(OPTO)Cl$ derivative **15** revealed even smaller downfield shifts of its ^{29}Si NMR signal from 25 to 40 °C in $CDCl_3$ and in toluene-d_8 ($\Delta\delta$ = 1.7 and 1.6 ppm, respectively) along with shifting of its ^{13}C OPTO ligand resonances in directions characteristic of π-electron localization. These observations indicate that the substantial increase in the strength of the Si—S bond, as assessed by the ^{13}C NMR C=S chemical shift (δ 157.0 ppm) and X-ray structure analysis, suppresses but does not completely inhibit thermally-induced Si←S bond dissociation.

Exploration of Hydrogen-bond Donor Interactions with Chloroform. Solvent-dependent ^{29}Si NMR chemical shifts were observed for **1**, **5**, **8**, **9**, and **15**. In all cases, resonances appeared consistently at lower field in $CDCl_3$ than in toluene-d_8 indicating a general weakening of chelate interactions in $CDCl_3$. The largest solvent effect was observed for **9** (δ = -55.4 ppm, toluene-d_8; δ = -32.9 ppm, $CDCl_3$).[52] Given the non-classical H-bonding O—H···S=C interactions that occur in the free HOPTO ligand[24] and in 1-hydroxy-4(1*H*)-pyridinethione,[53] weak H-bond donor interactions of chloroform with sulfur, oxygen, or both are possible. In an NMR tube study of **9** in toluene-d_8, incremental addition of small amounts of $CHCl_3$ resulted in unidirectional downfield ^{13}C NMR shifts of **a-e**.[54] Given the established pattern of ^{13}C NMR shifts that occur upon π-ED (vide infra), this observation is inconsistent with increased Si←S bond dissociation and therefore does not support an H-bond donor interaction of chloroform with sulfur.[55] Although solvent effects not due to H-bonding interactions can weaken ligand donor interactions with silicon,[56] we propose an H-bond donor interaction of chloroform with oxygen to explain the large solvent effect of the ^{29}Si NMR chemical shift of **9**. Such an interaction might be expected to result in increased π-ED toward *N*-oxide formation and in a strengthened Si-S bond, but this is not observed and suggests that the H-bond donor interaction leads instead toward protonolysis of the Si-O bond.

Solvent effects were probed similarly for the strongly chelated complex **15**. At room temperature in toluene-d_8, diastereotopic methyl groups are indicated in the ^{1}H and ^{13}C NMR spectra but are magnetically equivalent in neat $CDCl_3$ or CD_3CN. In an NMR tube experiment, incremental amounts of $CHCl_3$ up to 175 equiv. were added to a toluene-d_8 solution of **15** upon which the ^{1}H and ^{13}C methyl resonances coalesced (Figures S53 and S54), the ^{29}Si resonance shifted slightly downfield by 3.6 ppm, and the five ^{13}C OPTO resonances shifted downfield. These spectral changes are inconsistent with a shift in chelation equilibrium by Si←S bond dissociation. Ionization of the Si-Cl bond was also discounted on the basis of the same pattern of unidirectional shifts in the ^{13}C NMR spectrum of **15** observed for non-chlorinated **9** in a similar experiment,[57] and on limited reports of chloride ionization in 5-coordinate dialkyl organosilicon complexes of which their Si-Cl bonds are significantly longer than that of **15**.[58] Finally, a slight weakening of the chelate is indicated by the lower field ^{29}Si NMR signal, presumably from an H-bond donor interaction with oxygen, although an Si←O dative bond dissociation is not supported given that the same ^{13}C NMR pattern of shifts is observed for **9** which contains strong covalent Si-O bonds. The mechanism for the loss of topicity is therefore most consistent with a non-dissociative Berry process facilitated by an increase in solvent polarity.

In an additional NMR tube experiment of **15** in toluene-d_8, incremental amounts of CH_3CN up to 100 equiv. were added (Figure S55). The pairs of ^{1}H and ^{13}C methyl resonances coalesced, and the ^{29}Si resonance shifted slightly upfield by 2.8 ppm. The separation of ^{13}C resonances **b** and **d** gradually

decreased by 2.3 ppm and **a** shifted upfield by 2.3 ppm, both of which generally signal an increase in π-ED within the OPTO ligand, along with a downfield shift of **e** by 0.6 ppm. The same general pattern of differences can be seen in the spectra of the free HOPTO ligand in neat toluene-d_8 vs. neat CD_3CN among other solvents (Figure S56). This suggests that the ligand is solvated similarly in **15** leading to increased π-ED and increased chelate strength as given by the higher field ^{29}Si NMR shift.

In light of several known acetonitrile adducts of silyl cations,[59] the possibility of chloride displacement by CH_3CN in **15** was examined and ruled out as a possible mechanism for the observed stereodynamic process. In CD_3CN, the triflato derivative, $[^{i}Pr_2Si(OPTO)]^+[OSO_2CF_3]^-$ (**15a**), displays a ^{13}C NMR spectrum consistent with a strongly chelating OPTO ligand and a ^{29}Si NMR signal ~60 ppm downfield of that of **15** (δ +30.8 and −33.6 ppm, respectively). This characterizes **15a** as a separated ion pair with a 4-coordinate silicon complex cation. Consequently, an ion pair of **15** with dissociated chloride cannot be a CD_3CN adduct. Further, cooling of a saturated solution of **15** in neat CH_3CN resulted in crystallization of the non-adduct as determined by X-ray crystallographic analysis. As with added $CHCl_3$ described above, the loss of topicity upon addition of CH_3CN reflects an increase in the rate of a non-dissociative dynamic process that is facilitated likely by an increase in solvent polarity.[60]

Conclusion.

The characterization of a family of organosilicon pyrithione complexes has led to a clear relationship between the carbon-sulfur bond length, ^{13}C NMR C=S chemical shift, and chelate strength given by the Si-S bond length and O-Si-S bite angle. The range of carbon-sulfur bond lengths observed in these organosilicon complexes spans nearly the entire range of those of all structurally characterized transition-metal, rare-earth, and main group pyrithione complex structures currently in the CSD. X-ray structural data and variable-temperature ^{13}C NMR data of unchelated to strongly chelated organosilicon OPTO complexes shows that the extent of π-ED increases within the pyridine ring *in tandem* with increasing chelate strength along the **i** to **iii** continuum. Lower and upper limits of the carbon-sulfur bond lengths (~1.67 and 1.73 Å) and of the ^{13}C NMR C=S chemical shifts (δ ~154 to 176 ppm) in $CDCl_3$ both serve as useful signature markers of the approximate limits of chelate ring formation that should be applicable in assessing relative chelate strengths within other families of pyrithione metal complexes. For example, a survey of known organostannanes, $R_3Sn(OPTO)$ (R = Ph, Bn), $R_2Sn(OPTO)_2$ (R = Me, *n*-Bu, Ph, Bn), and $R_2Sn(OPTO)Cl$ (R = Me, Ph) reveals carbon-sulfur bond lengths ranging from 1.704-1.732 Å.[45,61] Variable-temperature ^{13}C NMR studies of chelated complexes additionally reveals Si←S bond dissociation equilibria occurring in solution. In the most strongly chelated complexes, despite effectively stronger Si-S bonds, Si←S bond dissociation is still evident within the limit of detection.

Complexes **3** and **11** display the pseudo-ambidentate potential of the OPTO ligand as the first examples of S_{ax} TBP isomers in the literature. In accord with simple bonding theory, the orientation of the chelated OPTO ligand across axial and equatorial sites in TBP complexes has been shown to influence the electronic character of its structure with S_{eq} isomers able to undergo π-ED to a greater extent than S_{ax} isomers.

Finally, a comparison of di- and tri-organosilicon OPTO vs. OPO complexes from our earlier work indicates an overall weaker chelate effect of the OPTO ligand with lower coordination numbers generally observed in their solid states: $Ph_3Si(OPTO)$ is 4-coordinated and $Ph_3Si(OPO)$ is 5-coordinated; $Me_2Si(OPTO)_2$ is 5-coordinated and $Me_2Si(OPO)_2$ is 6-coordinated; $^tBu_2Si(OPTO)_2$ is 4-coordinated and $^tBu_2Si(OPO)_2$ is 5-coordinated, and $(mesityl)_2Si(OPTO)_2$ is 4-coordinated and $(mesityl)_2Si(OPO)_2$ is 6-coordinated.[13a,62] We speculate the difference in chelate strength to be due qualitatively to the greater difference in electronegativity between oxygen and silicon than between sulfur and silicon which would be expected to increase the ionic character in the bonding. Further work in these and related complexes will involve computational studies to understand the charge distributions in these molecules and the energies associated with π-ED.

Acknowledgments.

The authors gratefully acknowledge NSF MRI program award #1828310 for the purchase of an NMR spectrometer, the University of Rochester and associated funding from NSF MRI program award CHE-1725028, and St. John Fisher University (formerly St. John Fisher College) Summer Fellows Research Program for support. We also thank Maria Camila Aguilera Cuenca for solving the X-ray structure of **6**, Brandon Wilson for solving the X-ray structure of **7**, and the many contributions to this work by the 2013-2015 classes of Advanced Lab II undergraduate students of St. John Fisher College.

Experimental Section.

General Considerations. All manipulations were performed inside a N_2-filled Vacuum Atmospheres glovebox and all reactions were carried out in amber glass vials to protect samples from ambient light. Pentane and tetrahydrofuran were dried and vacuum-distilled from purple solutions of benzophenone ketyl and stored over activated 4Å molecular sieves. Toluene, chloroform, and triethylamine were dried and vacuum distilled from activated 4Å molecular sieves. Silyl chlorides were purchased from Gelest, Inc. and used as received. Pyrithione (a.k.a. 2-Pyridinethiol 1-oxide) and DBU were purchased from Aldrich and used as received. ^1H, $^{13}C\{^1H\}$, and $^{29}Si\{^1H\}$ NMR spectra were recorded at 296 Kelvin using either a Bruker DPX250 NMR spectrometer (^1H, 250.1 MHz; ^{13}C, 62.9 MHz; ^{29}Si, 49.7 MHz) or a Bruker

Ascend400 NMR spectrometer (^{1}H, 400.15 MHz; ^{13}C 100.62 MHz; ^{29}Si, 79.50 MHz). ^{29}Si NMR spectra were recorded at a resolution of 0.36 Hz (DPX250) or 0.59 Hz (Ascend400). ^{1}H and ^{13}C NMR chemical shifts were determined relative to residual solvent protons in $CDCl_3$ (^{1}H, δ 7.26; ^{13}C, δ 77.16), CD_3CN (^{1}H, δ 1.94; ^{13}C, δ 118.26), and toluene-d_8 (^{1}H, δ 2.08; ^{13}C, δ 20.43), or to external TMS. ^{29}Si NMR chemical shifts were referenced to external TMS in the same solvent. Samples submitted for elemental analysis were obtained on recrystallized samples unless otherwise noted, and were analyzed at the CENTC Elemental Analysis Facility at the University of Rochester.

Single Crystal X-ray Crystallography.

*Structures **1-3, 7-12, 15-18**:* Crystals were placed onto the tips of glass optical fibers and mounted on a Bruker SMART platform diffractometer equipped with an APEX II CCD area detector for data collection.[63] For each, a preliminary set of cell constants and an orientation matrix were calculated from three orthogonal wedges of reciprocal space. Full data collections were carried out using a fine-focus sealed X-ray tube (MoKα radiation, 0.71073 Å) with frame times ranging from 25 to 90 seconds and a detector distance of approximately 40 mm. Randomly oriented regions of reciprocal space were surveyed: four to six major sections of frames were collected with 0.50º steps in ω at four to six different φ settings and a detector position of -38º in 2θ. The intensity data were corrected for absorption.[64] Final cell constants were calculated from the xyz centroids of approximately 4000 strong reflections from the actual data collections after integration.[65]

*Structures **6, 13, 19-20**:* Crystals were placed onto Nylon loops and mounted on a Rigaku XtaLAB Synergy-S diffractometer equipped with a HyPix-6000HE HPC area detector for data collection.[66] For each, a preliminary set of cell constants and an orientation matrix were calculated from a small random sampling of reflections, after which a short pre-experiment was run from which an optimal data collection strategy was determined. Full data collections were carried out using a PhotonJet microfocus X-ray source (CuKα radiation, 1.54184 Å) with frame times ranging from 0.09 to 1.89 seconds and a detector distance of 34.0 mm. Series of frames were collected in 0.50º steps in ω at different 2θ, κ, and φ settings. After the intensity data were corrected for absorption, the final cell constants were calculated from the xyz centroids of the strong reflections from the actual data collection after integration.

All structures: Structures were solved using SIR2011[67] (**1-3**, **8**, **11-12**, **15-18**), SHELXS[68] (**7**), or SHELXT[69] (**6**, **9-10**, **13**, **19-20**) and refined using SHELXL.[69] Space groups were determined based on systematic absences (**2-3**, **6**, **9-11**, **15-17**, **19**), intensity statistics (**8**, **12**), or both (**1**, **7**, **13**, **18**, **20**). Most or all non-hydrogen atoms were assigned from the solution. Full-matrix least squares / difference Fourier

cycles were performed which located any remaining non-hydrogen atoms. All non-hydrogen atoms were refined with anisotropic displacement parameters. All hydrogen atoms were placed in ideal positions and refined as riding atoms with relative isotropic displacement parameters. Full matrix least squares refinements on F^2 were run to convergence.

Structure manipulation and figure generation were performed using SHELXTL[68] (**1**-**3**, **7**-**12**, **15**-**18**) or Olex2[70] (**6**, **13**, **19**-**20**). The asymmetric unit of each structure contains one molecule in a general position, except for **8** and **11**, whose asymmetric units contain two independent molecules, and **13**, whose asymmetric unit contains one-half of a molecule on a crystallographic two-fold axis. In **7**, the propyl linkage of the silacycle is modeled as disordered over two positions (0.678(3):0.322(3)). In **12**, the allyl ligand is modeled as disordered over two positions (0.659(6):0.341(6)). In **13**, the bidentate ligand (one unique due to symmetry) is modeled as disordered with its monodentate isomer, which is found in two orientations relative to the bidentate ligand (0.923(2):0.030(2):0.047(2)). The pendant sulfur atom of the monodentate form was located in the difference Fourier map in two positions, corresponding to the two orientations. The $R1$ residual (strong data) increases from 5.13 to 6.34 % if the disorder is not modeled. In **16**, one allyl ligand is modeled as disordered over two positions (0.941(2):0.059(2)); when not modeled, $R1$ increases slightly, the two largest peaks of residual electron density are those pertaining to the disorder, and there are Hirshfeld test alerts for atom pairs Si1/C6 and C7/C8. For each disordered group or ligand, analogous bond lengths and angles were restrained to be similar and anisotropic displacement parameters for proximal atoms were restrained to be similar or constrained to be equivalent.

For **8**, the refinement stalled at $R1 = 0.069$, at which point twin modeling was required. After the non-merohedral twin law, [1 0 0 / -0.936 -1 0 / -0.055 0 -1], a 180 degree rotation about direct lattice [1 0 0], was determined, the data were re-integrated, and a new absorption correction was applied.[71] There were 7290 unique reflections solely in the first component, 7195 unique reflections solely in the second component, and 3912 unique overlapping reflections. The mass ratio of the two components refined to 0.8447(12):0.1553(12). For **9**, the refinement stalled at $R1 = 0.136$, at which point twin modeling was required. After the non-merohedral twin law, [1 0 0.529 / 0 -1 0 / 0 0 -1], a 180 degree rotation about reciprocal lattice [100], was determined, the data were re-integrated, and a new absorption correction was applied.[71] There were 1348 unique reflections solely in the first component, 1126 unique reflections solely in the second component, and 3788 unique overlapping reflections. The mass ratio of the two components refined to 0.7609(16):0.2391(16).

See Tables S1-S4 in the Supporting Information for additional structural details.

Me_3Si(OPTO) (1). To a stirred solution of pyrithione (0.262 g, 2.06 mmol) and NEt_3 (0.30 mL, 2.2 mmol) in THF (14 mL) was added Me_3SiCl (0.26 mL, $d = 0.858$ g/mL, 2.1 mmol) dropwise at room

temperature. The resulting mixture was stirred for 1 day and the NEt_3HCl salt was removed by filtration and washed once with 1 mL of THF. Removal of the solvent under vacuum afforded 0.381 g (93%) of a yellow powder. X-ray quality crystals were grown at room temperature from THF/pentane by the diffusion method. ^1H NMR ($CDCl_3$): δ 0.34 (s, 9H, $SiCH_3$), 6.54 (ddd, ^3J = 6.9, ^3J = 6.9, ^4J = 1.9 Hz, 1H, C*H*CHN), 7.04 (ddd, ^3J = 8.8, ^3J = 6.8, ^4J = 1.7 Hz, 1H, C*H*CHCS), 7.60-7.67 (m, 2H). ^{13}C NMR ($CDCl_3$): δ 0.2 ($SiCH_3$), 112.9 (*C*HCHN), 131.8 (*C*HCHCS), 137.1 (*C*HCS), 138.1 (CHN), 175.5 (CS). ^{29}Si NMR ($CDCl_3$): δ 39.8. Anal. Calcd for $C_8H_{13}NOSSi$: C, 48.20; H, 6.57; N, 7.02. Found: 48.31% C; 6.56% H; 7.09% N.

Ph_3Si(OPTO) (2). To a stirred solution of pyrithione (0.132 g, 1.04 mmol) and NEt_3 (0.15 mL, 1.1 mmol) in THF (8 mL) was added a solution of Ph_3SiCl (0.306 g, 1.04 mmol) in THF (2 mL) dropwise at room temperature. The resulting mixture was stirred for 1 day and the NEt_3HCl salt was removed by filtration and washed once with 1 mL of THF. Removal of the solvent under vacuum afforded 0.401 g (>99%) of a yellow-green powder. X-ray quality crystals were grown at room temperature from THF/pentane by the diffusion method. ^1H NMR ($CDCl_3$): δ 6.16 (ddd, ^3J = 6.9, ^3J = 6.9, ^4J = 1.9 Hz, 1H), 6.70 (ddd, ^3J = 8.9, ^3J = 6.7, ^4J = 1.6 Hz, 1H), 7.17-7.34 (m, 10H), 7.43-7.51 (m, 2H), 7.56-7.60 (m, 5H). ^{13}C NMR ($CDCl_3$): δ 112.3, 128.2, 130.6, 131.2, 131.3, 136.4, 137.3, 137.9, 176.0 (CS). ^{29}Si NMR ($CDCl_3$): δ 2.5. Anal. Calcd for $C_{23}H_{19}NOSSi$: C, 71.65; H, 4.97; N, 3.63. Found: C, 71.49; H, 4.91, N, 3.58.

Me_2Si(OPTO)$_2$ (3). To a stirred solution of pyrithione (0.329 g, 2.58 mmol) and NEt_3 (0.37 mL, 2.7 mmol) in THF (14 mL) was added Me_2SiCl_2 (0.15 mL, *d* = 1.06 g/mL, 1.2 mmol) dropwise at room temperature. The resulting mixture was stirred for 1 day and the NEt_3HCl salt was removed by filtration and washed once with 2 mL of THF. Removal of the solvent under vacuum afforded 0.358 g (89%) of a yellow powder. X-ray quality crystals were grown at room temperature from THF/pentane by the diffusion method. ^1H NMR ($CDCl_3$): δ 0.76 (s, 6H, $SiCH_3$), 6.74 (ddd, ^3J = 6.9, ^3J = 6.9, ^4J = 1.8 Hz, 2H), 7.22 (ddd, ^3J = 8.3, ^3J = 7.0, ^4J = 1.6 Hz, 2H), 7.67 (dd, ^3J = 8.6, ^4J = 1.6 Hz, 2H), 7.99 (dd, ^3J = 6.9, ^4J = 1.3 Hz, 2H). ^{13}C NMR ($CDCl_3$): δ 4.7 ($SiCH_3$), 114.7, 132.5, 133.7, 137.3, 170.1 (CS). ^{29}Si NMR ($CDCl_3$): δ −19.0. Anal. Calcd for $C_{12}H_{14}N_2O_2S_2Si$: C, 46.42; H, 4.55; N, 9.02. Found: C, 46.32; H, 4.50; 8.91.

Et_2Si(OPTO)$_2$ (4). To a stirred solution of pyrithione (0.302 g, 2.37 mmol) and NEt_3 (0.35 mL, 2.5 mmol) in THF (14 mL) was added Et_2SiCl_2 (0.18 mL, *d* = 1.05 g/mL, 1.2 mmol) dropwise at room temperature. The resulting mixture was stirred for 1 day and the NEt_3HCl salt was removed by filtration

and washed once with 1 mL of THF. Removal of the solvent with the assistance of light heating under vacuum afforded 0.397 g (99%) of a viscous yellow oil. Elemental analysis was performed without further purification. ^{1}H NMR ($CDCl_3$): δ 0.99-1.24 (m, 10H), 6.72 (ddd, ^{3}J = 6.9, ^{3}J = 6.9, ^{4}J = 1.8 Hz, 2H), 7.21 (ddd, ^{3}J = 7.9, ^{3}J = 6.9, ^{4}J = 1.6 Hz, 2H), 7.67 (dd, ^{3}J = 8.6, ^{4}J = 1.8 Hz, 2H), 7.98 (dd, ^{3}J = 6.9, ^{4}J = 1.4 Hz, 2H). ^{13}C NMR ($CDCl_3$): δ 7.7, 13.3, 114.4, 132.4, 133.5, 137.3, 170.3 (CS). ^{29}Si NMR ($CDCl_3$): δ –20.2. Anal. Calcd for $C_{14}H_{18}N_2O_2S_2Si$: C, 49.67; H, 5.36; N, 8.28. Found: C, 49.75; H, 5.41; N, 8.01.

^{i}Pr$_2$Si(OPTO)$_2$ (5). To a stirred solution of pyrithione (0.278 g, 2.19 mmol) and NEt_3 (0.32 mL, 2.3 mmol) in THF (14 mL) was added $^{i}Pr_2SiCl_2$ (0.20 mL, *d* = 1.03 g/mL, 1.1 mmol) dropwise at room temperature. The resulting mixture was stirred for 1 day and the NEt_3HCl salt was removed by filtration and washed once with 1 mL of THF. Removal of the solvent with the assistance of heating under vacuum afforded 0.411 g of a very viscous yellow oil. After 4 hours under vacuum with mild heating, removal of THF was incomplete and other impurities were observed in the NMR spectra. Elemental analysis was performed without further purification. ^{1}H NMR ($CDCl_3$): δ 1.10 (d, *J* = 7.3 Hz, 12H), 1.76 (sep, *J* = 7.3 Hz, 2H), 6.71 (ddd, ^{3}J = 7.0, ^{3}J = 7.0, ^{4}J = 1.9 Hz, 2H), 7.20 (ddd, ^{3}J = 7.9, ^{3}J = 6.9, ^{4}J = 1.4 Hz, 2H), 7.64 (dd, ^{3}J = 8.7, ^{4}J = 1.8 Hz, 2H), 7.99 (dd, ^{3}J = 6.7, ^{4}J = 1.4 Hz, 2H). ^{13}C NMR ($CDCl_3$): δ 18.4, 21.0, 144.4, 132.4, 133.0, 137.1, 169.8 (CS). ^{29}Si NMR ($CDCl_3$): δ –28.4. Anal. Calcd for $C_{16}H_{22}N_2O_2S_2Si$: C, 52.42; H, 6.05; N, 7.64. Found: C, 51.86; H, 6.16; N, 7.38.

^{t}Bu$_2$Si(OPTO)$_2$ (6). To a stirred solution of pyrithione (0.282 g, 2.22 mmol) and 1,8-diazabicyclo[4.5.0]undec-7-ene (DBU) (0.33 mL, *d* = 1.02 g/mL, 2.2 mmol) in THF (10 mL) was added $^{t}Bu_2SiCl_2$ (0.25 mL, *d* = 1.01 g/mL, 1.2 mmol) dropwise at room temperature. The resulting mixture was stirred for 1 day, filtered, and washed once with 1 mL of THF. The filtrate was dried under vacuum to afford 0.477 g of a pale yellow sticky powder. A portion (0.0881 g) was recrystallized from THF/pentane by diffusion to afford 0.0564 g (64%) of X-ray quality crystals. ^{1}H NMR ($CDCl_3$): δ 1.21 (s, 18H), 6.61 (ddd, ^{3}J = 6.8 Hz, ^{3}J = 6.8, ^{4}J = 1.6 Hz, 2H), 7.11 (br t, ^{3}J = 7.4 Hz, 2H), 7.66 (dd, ^{3}J = 8.7, ^{4}J = 1.9 Hz, 2H), 8.49 (br d, ^{3}J = 4.0 Hz, 2H). ^{13}C NMR ($CDCl_3$): δ 23.4 ($C(CH_3)_3$), 28.7 ($C(CH_3)_3$), 113.0, 132.0, 136.8, 138.8, 174.6 (CS). ^{29}Si NMR ($CDCl_3$): δ –2.6. Anal. Calcd for $C_{18}H_{26}N_2O_2S_2Si$: C, 54.78; H, 6.64; N, 7.10. Found: C, 54.67; H, 6.67; N, 7.29.

(CH$_2$)$_3$Si(OPTO)$_2$ (7). To a stirred solution of pyrithione (0.316 g, 2.48 mmol) and NEt_3 (0.36 mL, 2.6 mmol) in THF (14 mL) was added $(CH_2)_3SiCl_2$ (0.15 mL, *d* = 1.20 g/mL, 1.3 mmol) dropwise at room temperature. The resulting mixture was stirred for 1 day and the NEt_3HCl salt was removed by filtration

and washed once with 1 mL of THF. Removal of the solvent under vacuum afforded 0.345 g (86%) of a very sticky yellow residue. Recrystallization from THF/pentane by the diffusion method deposited crystals suitable only for X-ray analysis and could not be purified further due to co-precipitation of a sticky residue. ^{1}H NMR ($CDCl_3$): δ 1.53-1.75 (m, 6H), 6.86 (ddd, ^{3}J = 7.0, ^{3}J = 7.0, ^{4}J = 1.9 Hz, 2H), 7.31 (ddd, ^{3}J = 7.8, ^{3}J = 7.0, ^{4}J = 1.4 Hz, 2H), 7.49 (dd, ^{3}J = 8.4, ^{4}J = 1.6 Hz, 2H), 8.03 (dd, ^{3}J = 6.9, ^{4}J = 1.0 Hz, 2H). ^{13}C NMR ($CDCl_3$): δ 13.1 ($SiCH_2\mathit{C}H_2$), 38.7 ($SiCH_2$), 116.6, 128.7, 132.6, 135.3, 162.7 (CS). ^{29}Si NMR ($CDCl_3$): δ −111.7. Anal. Calcd for $C_{13}H_{14}N_2O_2S_2Si$: C, 48.42; H, 4.38; N, 8.69. Found: C, 47.96; H, 4.39; N, 8.14.

$(CH_2)_4Si(OPTO)_2$ (8). To a stirred solution of pyrithione (0.303 g, 2.38 mmol) and NEt_3 (0.35 mL, 2.5 mmol) in THF (14 mL) was added $(CH_2)_4SiCl_2$ (0.15 mL, *d* = 1.19 g/mL, 1.1 mmol) dropwise at room temperature. The resulting mixture was stirred for 1 day and the NEt_3HCl salt was removed by filtration and washed once with 1 mL of THF. Removal of the solvent under vacuum afforded 0.357 g (89%) of a white powder. X-ray quality crystals were grown at room temperature from THF/pentane by the diffusion method. ^{1}H NMR ($CDCl_3$): δ 0.53-0.58 (br m, 4H), 1.39-1.45 (br m, 4H), 6.72 (ddd, ^{3}J = 6.9, ^{3}J = 6.9, ^{4}J = 1.7 Hz, 2H, C*H*CHN), 7.12 (ddd, ^{3}J = 8.7, ^{3}J = 7.2, ^{4}J = 1.5 Hz, 2H, C*H*CHCS), 7.35-7.39 (m, 2H, CHCS), 7.84-7.88 (m, 2H, CHN). ^{13}C NMR ($CDCl_3$): δ 24.7, 25.6, 116.3 (*C*HCHN), 129.1 (*C*HCS), 132.4 (*C*HCHCS), 135.3 (CHN) 163.4 (CS). ^{29}Si NMR ($CDCl_3$): δ −80.2. Anal. Calcd for $C_{14}H_{16}N_2O_2S_2Si$: C, 49.97; H, 4.79; N, 8.32. Found: C, 49.96; H, 4.72; N, 8.33.

$(CH_2)_5Si(OPTO)_2$ (9). To a stirred solution of pyrithione (0.295 g, 2.32 mmol) and NEt_3 (0.34 mL, 2.4 mmol) in THF (12 mL) was added $(CH_2)_5SiCl_2$ (0.17 mL, *d* = 1.16 g/mL, 1.2 mmol) dropwise at room temperature. The resulting mixture was stirred for 1 day and the NEt_3HCl salt was removed by filtration. Removal of the solvent under vacuum afforded 0.417 g of a waxy oil. The oil was recrystallized from THF/pentane by the diffusion method, washed with pentane, and dried under vacuum to afford 0.348 g (87%) of yellow crystals that melted upon breaking the vacuum. X-ray quality crystals were grown at room temperature from THF/pentane by the diffusion method. ^{1}H NMR ($CDCl_3$): δ 1.28 (t, *J* = 6.4 Hz, 4H), 1.41-1.53 (m, 2H), 1.73-1.90 (m, 4H), 6.68 (ddd, ^{3}J = 6.9, ^{3}J = 6.9, ^{4}J = 1.7 Hz, 2H, C*H*CHN), 7.19 (ddd, ^{3}J = 7.9, ^{3}J = 7.7, ^{4}J = 1.4 Hz, 2H, C*H*CHCS), 7.58 (dd, ^{3}J = 8.4, ^{4}J = 1.6 Hz, 2H, CHCS), 7.83 (dd, ^{3}J = 6.6, ^{4}J = 1.2 Hz, 2H, CHN). ^{13}C NMR ($CDCl_3$): δ 22.4, 25.3, 28.9 ($SiCH_2CH_2\mathit{C}H_2$), 114.6 (*C*HCHN), 132.5 (*C*HCS), 132.8 (*C*HCHCS), 137.0 (CHN), 169.2 (CS). ^{29}Si NMR ($CDCl_3$): δ −32.9. Anal. Calcd for $C_{15}H_{18}N_2O_2S_2Si$: C, 51.40; H, 5.18; N, 7.99. Found: C, 51.15; H, 5.02; N, 7.79.

(mesityl)$_2$Si(OPTO)$_2$ (10). To a stirred solution of pyrithione (0.196 g, 1.54 mmol) and NEt_3 (0.24 mL, 1.7 mmol) in THF (8 mL) was added mesityl$_2$SiCl$_2$ (0.260 g, 0.771 mmol) dissolved in THF (2 mL) dropwise at room temperature. The resulting mixture was stirred for 1 day and the NEt_3HCl salt was removed by filtration. Removal of the solvent under vacuum afforded 0.425 g of a viscous yellow oil. A portion of the oil (0.0108 g) was recrystallized from THF/pentane by the diffusion method, washed with pentane, and dried under vacuum to afford 0.0078 g (72%) of yellow crystals. X-ray quality crystals were grown at room temperature from toluene/pentane by the diffusion method. ^{1}H NMR ($CDCl_3$): δ 2.22 (s, 6H), 2.53 (s, 12H), 6.27 (ddd, ^3J = 7.0, ^3J = 7.0, ^4J = 1.9 Hz, 2H), 6.92 (s, 4H), 6.95 (ddd, ^3J = 7.7, ^3J = 7.6, ^4J = 1.3 Hz, 2H), 7.54 (dd, ^3J = 8.6, ^4J = 1.9 Hz, 2H), 8.01 (dd, ^3J = 7.2, ^4J = 1.4 Hz, 2H). ^{13}C NMR ($CDCl_3$): δ 21.3, 24.9, 112.1, 125.1, 130.0, 131.7, 136.6, 138.8, 141.8, 145.2, 174.5 (CS). ^{29}Si NMR ($CDCl_3$): δ −16.9. Anal. Calcd for $C_{28}H_{30}N_2O_2S_2Si$: C, 64.83; H, 5.83; N, 5.40. Found: C, 64.73; H, 5.56; N, 5.19.

(allyl)$_2$Si(OPTO)$_2$ (11). To a stirred solution of pyrithione (0.291 g, 2.29 mmol) and NEt_3 (0.34 mL, 2.4 mmol) in THF (14 mL) was added (allyl)$_2$SiCl$_2$ (0.19 mL, d = 1.08 g/mL, 1.1 mmol) dropwise at room temperature. The resulting mixture was stirred for 1 day and the NEt_3HCl salt was removed by filtration and washed once with 1 mL of THF. Removal of the solvent under vacuum afforded 0.373 g (93%) of a yellow semi-solid residue. Crystals for X-ray analysis were grown at room temperature from THF/pentane by the diffusion method. ^{1}H NMR ($CDCl_3$): δ 2.30 (d, J = 8.1 Hz, 4H, $SiCH_2$), 4.77-4.90 (m, 4H, $SiCH_2CHCH_2$), 5.87-6.04 (m, $SiCH_2CH$), 6.84 (ddd, ^3J = 6.9, ^3J = 6.9, ^4J = 1.6 Hz, 2H), 7.31 (ddd, ^3J = 8.0, ^3J = 6.8, ^4J = 1.4 Hz, 2H), 7.66 (dd, ^3J = 8.5, ^4J = 1.6 Hz, 2H), 8.02 (dd, ^3J = 6.9, ^4J = 0.9 Hz, 2H). ^{13}C NMR ($CDCl_3$): δ 30.4 ($SiCH_2$), 114.3, 115.4, 131.7, 132.7, 134.8, 136.7, 167.1 (CS). ^{29}Si NMR ($CDCl_3$): δ −49.0. Anal. Calcd for $C_{16}H_{18}N_2O_2S_2Si$: C, 53.01; H, 5.00; N, 7.73. Found: C, 53.02; H, 5.08; N, 7.61.

Me(allyl)Si(OPTO)$_2$ (12). To a stirred solution of pyrithione (0.302 g, 2.37 mmol) and NEt_3 (0.35 mL, 2.5 mmol) in THF (14 mL) was added Me(allyl)SiCl$_2$ (0.17 mL, d = 1.08 g/mL, 1.2 mmol) dropwise at room temperature. The resulting mixture was stirred for 1 day and the NEt_3HCl salt was removed by filtration and washed once with 2 mL of THF. Removal of the solvent under vacuum afforded 0.349 g (87%) of a yellow powder. X-ray quality crystals were grown at room temperature from THF/pentane by the diffusion method. ^{1}H NMR ($CDCl_3$): δ 0.37 (s, 3H), 1.99 (d, J = 7.8 Hz, 2H), 4.46-4.60 (m, 2H), 5.54-5.72 (m, 1H), 6.54-6.59 (m, 2H), 7.01 (t, ^3J = 7.5 Hz, 2H), 7.38 (d, ^3J = 8.9 Hz, 2H), 7.78 (d, ^3J = 6.5 Hz, 2H). ^{13}C NMR ($CDCl_3$): δ 4.1 ($SiCH_3$), 30.1 ($SiCH_2$), 114.3 ($SiCH_2CHCH_2$), 115.4, 132.0, 132.5,

134.1 ($SiCH_2\underline{C}HCH_2$), 136.8, 167.5 (CS). ^{29}Si NMR ($CDCl_3$): δ −35.3. Anal. Calcd for $C_{14}H_{16}N_2O_2S_2Si$: C, 49.97; H, 4.79; N, 8.32. Found: C, 50.35; H, 4.70; N, 8.20.

(*p*-tolyl)$_2$Si(OPTO)$_2$ (13). To a solution of **1** (0.350 g, 1.76 mmol) in THF (10 mL) was added (*p*-tolyl)$_2SiCl_2$ (225 μL, *d* = 1.10 g/mL, 0.880 mmol) dropwise at room temperature. The mixture stirred for 1 day and the solvent was removed under vacuum. Three repetitions of the addition of THF (10 mL) and immediate removal of the volatiles under vacuum produced 0.429 g of a yellow powder. (*p*-tolyl)$_2$Si(OPTO)Cl (~23% by mass) remained in the sample by ^{1}H NMR integration of the methyl signals along with other impurities. Due to the complex mixture, complete NMR peak assignments could not be made. Crystals suitable for X-ray analysis were grown at room temperature from $CHCl_3$/THF by solvent layering in an NMR tube. ^{1}H NMR ($CDCl_3$): δ 2.24 (s), 2.31 (s), 2.34 (s), 2.38 (s), 6.56 (d), 6.59 (d), 6.62 (d), 7.09-7.26 (m), 7.51 (d), 7.55 (d), 7.72 (d of d), 7.81 (d). ^{13}C NMR ($CDCl_3$): δ 21.6, 115.6, 128.3, 128.4, 130.9, 132.3, 134.5, 135.1, 136.6, 137.5, 138.6, 166.0. ^{29}Si NMR ($CDCl_3$): δ −70.1, −67.1 (**17**).

Me$_2$Si(OPTO)Cl (14). To a stirred solution of pyrithione (0.231 g, 1.82 mmol) and NEt_3 (0.27 mL, 1.9 mmol) in THF (14 mL) was added Me_2SiCl_2 (0.22 mL, *d* = 1.06 g/mL, 1.8 mmol) dropwise at room temperature. The resulting mixture was stirred for 1 day and the NEt_3HCl salt was removed by filtration and washed once with 1 mL of THF. Removal of the solvent under vacuum afforded 0.318 g of a viscous yellow oil. NMR spectral data were consistent with $Me_2Si(OPTO)Cl$ containing a small amount of $Me_2Si(OPTO)_2$. An attempt to recrystallize the product from THF/pentane by diffusion at room temperature resulted in the isolation of the analytically pure redistribution product, $Me_2Si(OPTO)_2$. ^{1}H NMR ($CDCl_3$): δ 0.84 (s, 6H), 7.15 (br t, *J* = 6.7 Hz, 1H), 7.51-7.54 (br m, 1H), 7.57-7.60 (br m, 1H), 8.17 (br d, *J* = 6.6 Hz, 1H). ^{13}C NMR ($CDCl_3$): δ 11.0 ($SiCH_3$), 119.7, 126.0, 133.9, 134.7, 156.1 (CS). ^{29}Si NMR ($CDCl_3$): δ −36.6.

^{i}Pr$_2$Si(OPTO)Cl (15). To a stirred solution of pyrithione (0.184 g, 1.45 mmol) and NEt_3 (0.21 mL, 1.5 mmol) in THF (14 mL) was added $^iPr_2SiCl_2$ (0.26 mL, *d* = 1.03 g/mL, 1.4 mmol) dropwise at room temperature. The resulting mixture was stirred for 1 day and the NEt_3HCl salt was removed by filtration and washed once with 1 mL of THF. Removal of the solvent under vacuum afforded 0.386 g (>99%) of a pale yellow powder. X-ray quality crystals were grown at room temperature from THF/pentane by the diffusion method. ^{1}H NMR (CD_3CN): δ 1.09 (d, *J* = 7.3 Hz, 12H, CH_3), 1.44 (sep, *J* = 7.3 Hz, 2H, CH), 7.27-7.30 (m, 1H), 7.64-7.66 (m, 2H), 8.35 (dt, *J* = 6.6, *J* = 0.9 Hz, 1H). ^{13}C NMR (CD_3CN): δ 19.1 (br, CH_3), 23.9, 122.1, 125.6, 135.6, 135.8, 154.0 (CS). ^{29}Si NMR (CD_3CN): δ −33.6. ^{1}H NMR ($CDCl_3$): δ 1.12 (d, *J* = 7.3 Hz, 12H, CH_3), 1.54 (sep, *J* = 7.3 Hz, 2H, CH), 7.10 (ddd, ^3J = 7.0, ^3J = 7.0, ^4J = 1.8 Hz,

1H, C*H*CHN), 7.48 (ddd, ^3J = 8.7, ^3J = 7.1, ^4J =1.4 Hz, 1H, C*H*CHCS), 7.59 (dd, ^3J =8.4, ^4J = 1.8 Hz, 1H, CHCS), 8.19 (dd, J = 6.6, J = 1.4 Hz, 1H, CHN). ^{13}C NMR ($CDCl_3$): δ 18.7 (br), 22.8, 119.2 (*C*HCHN), 126.2 (*C*HCS), 133.3 (*C*HCHCS), 134.5 (CHN), 157.0 (CS). ^{29}Si NMR ($CDCl_3$): δ –26.1. Anal. Calcd for $C_{11}H_{18}ClNOSSi$: C, 47.89; H, 6.58; N, 5.08. Found: C, 48.01; H, 6.43; N, 5.32.

^{i}Pr$_2$Si(OPTO)(OSO$_2$CF$_3$) (15a). To a stirred solution of **15** (0.150 g, 0.544 mmol) in $CHCl_3$ (5 mL) was added $Me_3SiOSO_2CF_3$ (98.6 μL, d = 1.23 g/mL, 0.543 mmol) at room temperature and stirred for 1 hour. Removal of the volatiles under vacuum afforded 0.219 g of a yellow oil. Elemental analysis was performed without further purification. ^{1}H NMR (CD_3CN): δ 1.17 (br s, 12H, CH_3), 1.66 (sep, J = 7.5 Hz, 2H, CH), 7.58 (ddd, ^3J = 6.7, ^3J = 6.7, ^4J = 2.8 Hz, 1H), 7.95-8.00 (m, 2H), 8.60-8.62 (m, 1H). ^{13}C NMR (CD_3CN): δ 17.0 (br, CH_3), 17.4 (br, CH_3), 17.9, 124.2, 128.0, 137.8, 140.0, 152.9 (CS). ^{29}Si NMR (CD_3CN): δ 30.8. ^{1}H NMR ($CDCl_3$): δ 1.11 (d, J = 7.3 Hz, 12H, CH_3), 1.58 (sep, J = 7.3 Hz, 2H, CH), 7.32-7.36 (m, 1H), 7.74-7.76 (m, 2H), 8.42-8.44 (m, 1H). ^{13}C NMR ($CDCl_3$): δ 17.6 (CH_3), 20.1, 120.7, 126.9, 135.2, 136.5, 156.2 (CS). The expected ^{13}C NMR quartet of the triflate ion could not be located in either solvent, presumably broadened due to fluxional behavior. ^{29}Si NMR ($CDCl_3$): δ –8.6. Anal. Calcd for $C_{12}H_{18}F_3NO_4S_2Si$: C, 37.00; H, 4.66; N, 3.91. Found: C, 36.74; H, 4.57; N, 3.59.

(allyl)$_2$Si(OPTO)Cl (16). To a stirred solution of pyrithione (0.186 g, 1.47 mmol) and NEt_3 (0.22 mL, 1.6 mmol) in THF (14 mL) was added $(allyl)_2SiCl_2$ (0.25 mL, d = 1.08 g/mL, 1.5 mmol) dropwise at room temperature. The resulting mixture was stirred for 1 day and the NEt_3HCl salt was removed by filtration and washed once with 1 mL of THF. Removal of the solvent under vacuum afforded 0.261 g (66%) of a pale yellow powder. X-ray quality crystals were grown at room temperature from THF/pentane by the diffusion method. ^{1}H NMR ($CDCl_3$): δ 2.09 (d, J = 8.0 Hz, 4H), 4.63-4.79 (m, 2H), 5.75-5.92 (m, 4H), 7.05-7.13 (m, 1H), 7.40-7.48 (m, 2H), 8.06-8.10 (m, 1H). ^{13}C NMR ($CDCl_3$): δ 33.4 ($SiCH_2$), 114.2, 120.5, 124.9, 134.2, 134.6, 154.1 (CS). One carbon resonance of the allyl group is coincident with a carbon resonance of the OPTO ligand. ^{29}Si NMR ($CDCl_3$): δ –50.1. Anal. Calcd for $C_{11}H_{14}ClNOSSi$: C, 48.60; H, 5.19; N, 5.15. Found: C, 48.39; H, 5.20; N, 5.03.

(*p*-tolyl)$_2$Si(OPTO)Cl (17). To a stirred solution of pyrithione (0.137 g, 1.08 mmol) and NEt_3 (0.16 mL, 1.2 mmol) in THF (12 mL) was added $(p\text{-tolyl})_2SiCl_2$ (0.28 mL, d = 1.10 g/mL, 1.1 mmol) dropwise at room temperature. The resulting mixture was stirred for 1 day and the NEt_3HCl salt was removed by filtration and washed once with 1 mL of THF. Removal of the solvent under vacuum afforded 0.386 g (97%) of a pale yellow powder. A portion of the solid (0.099 g) was recrystallized from THF/pentane by the diffusion method, washed with pentane, and dried under vacuum to afford 0.062 g (63%) of pale

yellow crystals. Crystals for X-ray analysis were grown at room temperature from THF/pentane by the diffusion method. ^{1}H NMR ($CDCl_3$): δ 2.34 (s, 6H, CH_3), 7.08-7.14 (m, 1H), 7.17 (d, J = 7.8 Hz, 4H), 7.48-7.65 (m, 2H), 7.81 (d, J = 7.9 Hz, 4H), 8.16 (d, J = 6.5 Hz, 1H) ^{13}C NMR ($CDCl_3$): δ 21.6 (CH_3), 120.5, 125.0, 128.4, 134.2, 134.5, 134.5, 137.8, 139.1, 154.5 (CS). ^{29}Si NMR ($CDCl_3$): δ −65.6. Anal. Calcd for $C_{19}H_{18}ClNOSSi$: C, 61.35; H, 4.88; N, 3.77. Found: C, 60.97; H, 4.84; N, 3.75.

(mesityl)$_2$Si(OPTO)Cl (18). To a stirred solution of pyrithione (0.119 g, 0.935 mmol) and NEt_3 (0.14 mL, 1.0 mmol) in THF (8 mL) was added a solution of (mesityl)$_2SiCl_2$ (0.315 g, 0.934 mmol) in THF (2 mL) dropwise at room temperature. The resulting mixture was stirred for 1 day and the NEt_3HCl salt was removed by filtration and washed once with 1 mL of THF. Removal of the solvent under vacuum afforded 0.311 g (78%) of a yellow waxy solid. A portion of the solid (0.101 g) was recrystallized from THF/pentane by the diffusion method, washed with pentane, and dried under vacuum to afford 0.059 g (58%) of yellow crystals. Crystals for X-ray analysis were grown at room temperature from THF/pentane by the diffusion method. ^{1}H NMR ($CDCl_3$): δ 2.25 (s, 6H), 2.52 (s, 12H), 6.82-6.89 (m, 5H), 7.32 (ddd, ^{3}J = 8.7, ^{3}J = 7.1, ^{4}J = 1.3 Hz 1H), 7.59 (dd, ^{3}J = 8.5, ^{4}J = 1.6 Hz, 1H), 7.89 (dd, ^{3}J = 6.7, ^{4}J = 1.0 Hz, 1H). ^{13}C NMR ($CDCl_3$): δ 21.1, 24.4, 117.0, 129.9, 130.0, 133.2, 134.9, 135.8, 139.3, 143.5, 163.3 (CS). ^{29}Si NMR ($CDCl_3$): δ −44.1. Anal. Calcd for $C_{23}H_{26}ClNOSSi$: C, 64.53; H, 6.12; N, 3.27. Found: C, 64.57; H, 6.19; N, 3.15.

Ph$_2$Si(OPTO)Cl (19). To a solution of **1** (0.150 g, 0.752 mmol) in $CHCl_3$ (2 mL) was added Ph_2SiCl_2 (160 μL, d = 1.22 g/mL, 0.772 mmol) dropwise at room temperature upon which a precipitate formed immediately. The resulting mixture was stirred for 30 minutes and dried under vacuum for 2.5 hours to yield 0.270 g of a yellow powder. The resulting solid could not be dissolved fully in $CDCl_3$ with gentle heating and unidentified impurities were observed in the NMR spectra. Recrystallization of 186 mg of solid from $CHCl_3$/pentane by the diffusion method afforded a quantity of crystals sufficient only for X-ray structure determination. Efforts to isolate a pure specimen of **19** for elemental analysis were unsuccessful. Due to the complex mixture, complete peak assignments could not be made. ^{1}H NMR ($CDCl_3$): δ 7.13 (t), 7.35 (m), 7.53 (m), 7.75 (d), 7.91 (m), 8.16 (d). ^{13}C NMR ($CDCl_3$): δ 120.6, 125.0, 127.6, 128.5, 129.2, 131.9, 134.2, 134.3, 134.5, 141.2, 154.3. ^{29}Si NMR ($CDCl_3$): δ −66.8.

Supporting Information

Crystallographic tables, CIFs, NMR spectra. This material is available free of charge via the Internet at http://pubs.acs.org.

Author Information

Corresponding Author

* E-mail: bkraft@sjfc.edu

Notes

The authors declare no competing financial interest.

References

(1) For reviews on organosilicon complexes and their applications, see
(a) Klare, H. F. T.; Albers, L.; Süsse, L.; Keess, S.; Müller, T.; Oestreich, M. "Silylium Ions: From Elusive Reactive Intermediates to Potent Catalysts" *Chem. Rev.* **2021**, *121*, 5889. (b) Lemière, G.; Millanvois, A.; Ollivier, C.; Fensterbank, L. "A Parisian Vision of the Chemistry of Hypercoordinated Silicon Derivatives" *Chem. Rec.* **2021**, *21*, 1119. (c) Komiyama, T.; Minami, Y.; Hiyama, T. "Recent Advances in Transition-Metal-Catalyzed Synthetic Transformations of Organosilicon Reagents" *ACS Catal.* **2017**, *7*, 631. (d) Rossi, S.; Denmark, S. E. *Lewis Base Catalysis in Organic Synthesis*, Wiley-VCH Verlag GmbH&Co. KGaA, **2016**; p 1039. (e) Vlasova, N. N.; Sorokin, M. S.; Oborina, E. N. "Carbofunctional sulfur-containing organosilicon compounds" *Appl. Organometal. Chem.* **2017**, *31*, e3668. (f) Peloquin, D. M.; Schmedake, T. A. "Recent advances in hexacoordinate silicon with pyridine-containing ligands: Chemistry and emerging applications" *Coord. Chem. Rev.* **2016**, *323*, 107. (g) Nikolin, A. A.; Negrebetsky, V. V. "Synthesis, properties and reactivity of intramolecular hypercoordinate silicon complexes" *Russ. Chem. Rev.* **2014**, *83*, 848. (h) Wagler, J.; Böhme, U.; Kroke, E. "Higher-Coordinated Molecular Silicon Compounds" *Struct. Bond.* **2014**, *155*, 29. (i) Rendler, S.; Oestreich, M. "Hypervalent Silicon as a Reactive Site in Selective Bond-Forming Processes" *Synthesis* **2005**, *11*, 1727. (j) Tacke, R.; Ribbeck, T. "Bis(amidinato)and bis(guanidinato) silylenes and silylenes with one sterically demanding amidinato or guanidinato ligand: Synthesis and reactivity" *Dalton Trans.* **2017**, *46*, 13628. (k) Tacke, R.; Seiler, O. In *Silicon Chemistry: From the Atom to Extended Systems*; Jutzi, P., Schubert, U., Eds.; Wiley-VCH: Weinheim, Germany, 2003; p 324. (l) Brook, M. A. *Silicon in Organic Organometallic and Polymer Chemistry*; Wiley: New York, 2000; p 97. (m) Kira, M.; Zhang, L.-C. *The Chemistry of Hypervalent Compounds*; Akiba, K.-Y., Ed.; Wiley-VCH: Weinheim, Germany, 1999; p 147. (n) Tacke, R.; Pülm, M.; Wagner, B. "Zwitterionic pentacoordinate silicon compounds" *Adv. Organomet. Chem.* **1999**, *44*, 221. (o) Chuit, C.; Corriu, R. J. P.; Reyé, C.; Young, J. C. In *Chemistry of Hypervalent Compounds*; Akiba, K.-Y., Ed.; Wiley-VCH: New York, 1999; p 81. (p) Bassindale, A. R.; Glynn, S. J.; Taylor, P. G. In *The Chemistry of Organic Silicon Compounds*; Rappoport, Z.; Apeloig, Y., Eds.; Wiley: Chichester, U.K., 1998; vol. 2, part 1, p 495. (q) Kost, D.; Kalikhman, I. In *The Chemistry of Organic Silicon Compounds*; Rappoport, Z.; Apeloig, Y., Eds.; Wiley: Chichester, U.K., 1998; vol. 2, p 1339. (r) Holmes, R. R. "Comparison of phosphorus and silicon: Hypervalency, stereochemistry, and reactivity" *Chem. Rev*. **1996**, *96*, 927. (s) Chuit, C.; Corriu, R. J. P.; Reye, C.; Young, J. C. "Reactivity of penta- and hexacoordinate silicon compounds and their role as reaction intermediates" *Chem. Rev.* **1993**, *93*, 1371. (t) Holmes, R. R. "The stereochemistry of nucleophilic substitution of tetracoordinate silicon" *Chem. Rev.* **1990**, *90*, 17.

(2) For recent contributions to the field of hypercoordinate organosilicon chemistry, see: (a) Cruz-López, J. F.; Palacios-Chavez, J. A.; Guajardo-García, J. A.; González-García, A.; Báez, J. E.; López, J. A.;

Orozco-Castellanos, L. M.; González-García, G. "A straightforward synthesis of neutral hexacoordinated silicon (IV) complexes with SiN6 skeleton" *Inorg. Chim. Acta* **2021**, *523*, 120406. (b) Herbig, M.; Scholz, H.; Böhme, U.; Günther, B.; Gevorgyan, L.; Gerlach, D.; Wagler, J.; Schwarzer, S.; Kroke, E. "New cyclic and spirocyclic aminosilanes" *Main Group Met. Chem.* **2021**, *44*, 51. (c) Furuta, S.; Mori, T.; Yoshigoe, Y.; Sekine, K.; Kuninobu, Y. "Synthesis, structures and photophysical properties of hexacoordinated organosilicon compounds with 2-(2-pyridyl) phenyl groups" *Org. Biomol. Chem.* **2020**, *18*, 3239. (d) Kowalke, J.; Wagler, J.; Viehweger, C.; Brendler, E.; Kroke, E. "Ionic Dissociation of $SiCl_4$: Formation of $[SiL_6]Cl_4$ with L=Dimethylphosphinic Acid" *Chem. Eur. J.* **2020**, *26*, 8003. (e) Levernier, E.; Lévêque, C.; Derat, E.; Fensterbank, L.; Ollivier, C. "Towards Visible-Light Photocatalytic Reduction of Hypercoordinated Silicon Species" *Helv. Chim. Acta* **2020**, *103*, e1900238. (f) Viehweger, C.; Kowalke, J.; Brendler, E.; Schwarzer, S.; Vogt, C.; Kroke, E. "Five-and six-fold coordinated silicon in silicodiphosphonates: short range order investigation by solid-state NMR spectroscopy" *New J. Chem.* **2020**, *44*, 4613. (g) Ehrlich, L.; Gericke, R.; Brendler, E.; Wagler, J. "(2-Pyridyloxy)silanes as Ligands in Transition Metal Coordination Chemistry" *Inorganics* **2018**, *6*, 119. (h) Baus, J. A.; Tacke, R. "Neutral six-coordinate bis(dithiocarbamato)silicon(iv) complexes with an $SiCl_2S_4$ skeleton" *Dalton Trans.* **2017**, *46*, 8751. (i) Baus, J. A.; Laskowski, N.; Tacke, R. "A Silacyclopropene with a Six-Coordinate Silicon Atom and an SiN4C2 Skeleton: Synthesis and Structural Characterization" *Eur. J. Inorg. Chem.* **2016**, *33*, 5182. (j) Henker, J.; Wirmer-Bartoschek, J.; Bendel, L. E.; Xiang, Y.; Fu, C.; Harms, K.; Schwalbe, H.; Meggers, E. "Progress in the synthesis and bioactivity of hexacoordinate silicon (IV) complexes" *Eur. J. Inorg. Chem.* **2016**, *32*, 5161. (k) Mück, F. M.; Baus, J. A.; Bertermann, R.; Burschka, C.; Tacke, R. "Lewis Acid/Base Reactions of the Bis(amidinato)silylene $[^iPrNC(Ph)NiPr]_2Si$ and Bis(guanidinato)silylene $[^iPrNC(NiPr_2)NiPr]_2Si$ with $ElPh_3$ (El = B, Al)" *Organometallics* **2016**, *35*, 2583. (l) Mück, F. M.; Baus, J. A.; Burschka, C.; Tacke, R. "Cationic Five-Coordinate Bis(guanidinato)silicon(IV) Complexes with SiN4El Skeletons (El=S, Se): "Heterolytic Activation" of S−S and Se−Se Bonds" *Chem. Eur. J.* **2016**, *22*, 5830. (m) Baus, J. A.; Burschka, C.; Bertermann, R.; Guerra, C. F.; Bickelhaupt, F. M.; Tacke, R. "Neutral Six-Coordinate and Cationic Five-Coordinate Silicon(IV) Complexes with Two Bidentate Monoanionic N,S-Pyridine-2-thiolato(−) Ligands" *Inorg. Chem.* **2013**, *52*, 10664.

(3) Slone, C. S.; Weinberger, D. A.; Mirkin, C. A. "The transition metal coordination chemistry of hemilabile ligands" In *Progress in Inorganic Chemistry*; Wiley, **2007**; vol. 48, p 233.

(4) For related studies of organosilicon complexes of this type, see: (a) Qin, T.; Johnson, R. P.; Porco, J. A. Jr. "Vinylogous Addition of Siloxyfurans to Benzopyryliums: A Concise Approach to the Tetrahydroxanthone Natural Products" *J. Am. Chem. Soc.* **2011**, *133*, 1714. (b) Aksamentova, T. N.; Chipanina, N. N.; Voronkov, M. G.; Grebneva, E. A.; Albanov, A. I.; Trofimova, O. M.; Mukha, S. A.; Sukhov, B. G. "Synthesis and structure of (C= O→ Si← O′= C′) bis(2-methyl-4-oxopyran-3-yloxy) difluoro-(λ6) siliconium" *Russ. J. Gen. Chem.* **2009**, *79*, 98. (c) Voronkov, M. G.; Korlyukov, A. A.; Zel'bst, E. A.; Grebneva, E. A.; Trofimova, O. M.; Antipin, M. Yu. "Unusual molecular structure of (C= O→ Si← O′= C′) bis(2-methyl-4-pyrone-3-oxy) difluoro (λ6) siliconium" *J. Struct. Chem.* **2009**, *50*, 1204. (d) Tacke, R.; Burschka, C.; Willeke, M.; Willeke, R. "Neutral Mononuclear and Binuclear Hexacoordinate Silicon Complexes with SiO_5C Skeletons" *Eur. J. Inorg. Chem.* **2001**, *7*, 1671. (e) Tacke, R.; Willeke, M.; Penka, M. "Synthesis and Structural Characterization of Cationic Complexes with Hexacoordinate Silicon (IV) and Three Bidentate 1-Oxopyridine-2-olato (1–) Ligands" *Z. Anorg. Allg. Chem.* **2001**, *627*, 1236. (f) Azuma, S.; Kojima, M.; Yoshikawa, Y. "Stereochemistry of six-coordinated silicon complexes V1. Racemization and geometrical isomerization of tris (4-isopropyltropolonato) silicon (IV)" *Inorg. Chim. Acta* **1998**, *271*, 24. (g) Kira, M.; Zhang, L. C.; Kabuto, C.; Sakurai, H. "Synthesis and Structure of Hexacoordinate Organosilicon Compounds Having Tropolonato Ligands" *Chem. Lett.* **1995**, *8*, 659. (h) Evans, D. F.; Wong, C. Y. "Synthesis of new six-coordinate complexes of silicon (IV)" *Polyhedron* **1991**, *10*, 1131. (i) Inoue, T. "Kinetics of the racemization of tris(tropolonato) silicon (IV) perchlorate in organic solvents" *Inorg. Chem.* **1983**, *22*,

2435. (j) Weiss, A.; Harvey, D. R. "Wasserbeständige, kationische Siliciumkomplexe mit 1-Hydroxypyridin-N-oxyd" *Angew. Chem.* **1964**, *76*, 818; "Water-Stable, Cationic Complexes of Silicic Acid with 1-Hydroxypyridine N-Oxide" *Angew. Chem. Int. Ed. Engl.* **1964**, *3*, 698.

(5) (a) Kleinpeter, E.; Koch, A. "Chelatoaromaticity—existing: yes or no? An answer given by spatial magnetic properties (through space NMR shieldings—TSNMRS)" *Phys. Chem. Chem. Phys.* **2011**, *13*, 20593. (b) Zborowski, K. K.; Solà, M.; Poater, J.; Proniewicz, L. M. "Theoretical studies on aromaticity of selected hydroxypyrones. Part 3#. Chelatoaromaticity phenomenon in metalcomplexes of hydroxypyrones" *J. Phys. Org. Chem.* **2011**, *24*, 499. (c) Zborowski, K. K.; Proniewicz, L. M. "The Importance of Aromatic Effects for Metal Complexes Stabilization" In *New Trends in Coordination, Bioinorganic, and Applied Inorganic Chemistry*, Melnik, M., Segl'a, P., Tatarko, M., Eds.; Slovak University of Technology: Bratislava, 2011; p 601.

(6) (a) Zhang, Z.; Lyster, D. M.; Webb, G. A.; Orvig, C. "Potential ^{67}Ga radiopharmaceuticals for myocardial imaging: Tris(1-aryl-3-hydroxy-2-methyl-4-pyridinonato)gallium(III) complexes" *Nucl. Med. Biol.* **1992**, *19*, 327. (b) Nepveu, F.; Jasanada, F.; Walz, L. "Structural characterization of two lipophilic tris (tropolonato) gallium (III) and indium (III) complexes of radiopharmaceutical interest" *Inorg. Chim. Acta* **1993**, *211*, 141.

(7) (a) Martin, D. P.; Blachly, P. G.; McCammon, J. A.; Cohen, S. M. "Exploring the influence of the protein environment on metal-binding pharmacophores" *J. Med. Chem.* **2014**, *57*, 7126. (b) Jacobsen, F. E.; Breece, R. M.; Myers, W. K.; Tierney, D. L.; Cohen, S. M. "Model complexes of cobalt-substituted matrix metalloproteinases: Tools for inhibitor design" *Inorg. Chem.* **2006**, *45*, 7306. (c) Puerta, D. T.; Cohen, S. M. "Examination of novel zinc-binding groups for use in matrix metalloproteinase inhibitors" *Inorg. Chem.* **2003**, *42*, 3423.

(8) Grillo, A. S.; SantaMaria, A. M.; Kafina, M. D.; Cioffi, A. G.; Huston, N. C.; Han, M.; Seo, Y. A.; Yien, Y. Y.; Nardone, C.; Menon, A. V.; Fan, J.; Svoboda, D. C.; Anderson, J. B.; Hong, J. D.; Nicolau, B. G.; Subedi, K.; Gewirth, A. A.; Wessling-Resnick, M.; Kim, J.; Paw, B. H.; Burke, M. D. "Restored iron transport by a small molecule promotes absorption and hemoglobinization in animals" *Science* **2017**, *356*, 608.

(9) Finnegan, M. M.; Lutz, T. G.; Nelson, W. O.; Smith, A.; Orvig, C. "Neutral water-soluble post-transition-metal chelate complexes of medical interest: aluminum and gallium tris (3-hydroxy-4-pyronates)" *Inorg. Chem.* **1987**, *26*, 2171.

(10) (a) Thompson, K. H.; Orvig, C. "Vanadium compounds in the treatment of diabetes" *Met. Ions Biol. Syst.* **2004**, *41*, 221. (b) Melchior, M.; Rettig, S. J.; Liboiron, B. D.; Thompson, K. H.; Yuen, V. G.; McNeill, J. H.; Orvig, C. "Insulin-enhancing vanadium (III) complexes" *Inorg. Chem.* **2001**, *40*, 4686.

(11) (a) Wang, X.; Dai, X.; Shi, C.; Wan, J.; Silver, M. A.; Zhang, L.; Chen, L.; Yi, X.; Chen, B.; Zhang, D.; Yang, K.; Diwu, J.; Wang, J.; Xu, Y.; Zhou, R.; Chai, Z.; Wang, S. "A 3, 2-hydroxypyridinone-based decorporation agent that removes uranium from bones in vivo" *Nat. Commun.* **2019**, *10*, 1. (b) Szigethy, G.; Raymond, K. N. "Hexadentate terephthalamide (bis-hydroxypyridinone) ligands for uranyl chelation: structural and thermodynamic consequences of ligand variation" *J. Am. Chem. Soc.* **2011**, *133*, 7942. (c) Kim, J. E.; Bogart, J. A.; Carroll, P. J.; Schelter, E. J. "Rare earth metal complexes of bidentate nitroxide ligands: Synthesis and electrochemistry" *Inorg. Chem.* **2016**, *55*, 775. (d) Lewis, J. A.; Cohen, S. M. "Addressing lead toxicity: complexation of lead (II) with thiopyrone and hydroxypyridinethione O, S mixed chelators" *Inorg. Chem.* **2004**, *43*, 6534.

(12) (a) Angell, S. E.; Rogers, C. W.; Zhang, Y.; Wolf, M. O.; Jones Jr., W. E. "Hemilabile coordination complexes for sensing applications" *Coord. Chem. Rev.* **2006**, *250*, 1829. (b) Fenton, K. R.; Nagasubramanian, G.; Staiger, C.; Pratt, H.; Leung, K.; Rempe, S.; Chaudhari, M.; Anderson, T. M. "Organosilicon-based electrolytes for long-life lithium primary batteries" *U.S. Pat. Appl. Publ.* **2017**, US 20170207485 A1 20170720.

(13) (a) Kraft, B. M.; Brennessel, W. W. "Chelation and stereodynamic equilibria in neutral hypercoordinate organosilicon complexes of 1-hydroxy-2-pyridinone" *Organometallics* **2014**, *33*, 158. (b) Koch, J. G.; Brennessel, W. W.; Kraft, B. M. "Neutral and Cationic Bis-Chelate Monoorganosilicon (IV) Complexes of 1-Hydroxy-2-pyridinone" *Organometallics* **2017**, *36*, 594. (c) Kraft, B. M.; Brennessel, W. W.; Ryan, A. E.; Benjamin, C. K. "Crystal structures of tris-[1-oxo-pyridine-2-olato(1-)]silicon(IV) chloride chloro-form-d1 disolvate, tris-[1-oxo-pyridine-2-olato(1-)]silicon(IV) chloride aceto-nitrile unqu-anti-fied solvate, and fac-tris-[1-oxo-pyridine-2-thiol-ato(1-)]silicon(IV) chloride chloro-form-d1 disolvate" *Acta Crystallogr. Sect. E: Cryst. Commun.* **2015**, *71*, 1531.

(14) Other less common acronyms in the literature for the 2-pyrithione ligand include PT, PNO, mpo, and hqo.

(15) Two related organosilicon complexes, $Me_2(^tBu)Si(OPTO)$ and $Ph_3Si(OPTO)$, are reported in the literature but were not isolated nor characterized. See Barton, D. H. R.; Jaszberenyi, J. Cs.; Morrell, A. I. "The generation and reactivity of oxygen centered radicals from the photolysis of derivatives of N-hydroxy-2-thiopyridone" *Tet. Lett.* **1991**, *32*, 311.

(16) (a) Jones, R. A.; Katritzky, A. R. "N-Oxides and Related Compounds. Part XVII. The Tautomerism of Mercapto- and Acylamino-pyridine 1 -Oxides" *J. Chem. Soc.* **1960**, 2937. (b) Katritzky, A. R.; Jones, R. A. *"Infrared Absorption of Heteroaromatic and Benzenoid Six-membered Monocyclic Nuclei. Part X. Pyridones and Pyridthiones" J. Chem. Soc.* **1960**, 2947. (c) Kaszynski, P. "Tautomerism and Regioselectivity of Acylation of 4-Hydroxy-2-mercaptopyridine-N-oxide and 2,4-Dimercaptopyridine-N-oxide: A Computational Study" *Phosphorus, Sulfur, Silicon Relat. Elem.* **2009**, *184*, 1296. (d) Aveline, B. M.; Redmond, R. W. "Selective Photoexcitation of the Thione and Thiol Forms of N-Hydroxypyridine-4(*1H*)-Thione: A Tautomeric Heteroaromatic System" *J. Am. Chem. Soc.* **1999**, *121*, 9977.

(17) Groom, C. R.; Bruno, I. J.; Lightfoot, M. P.; Ward, S. C. "The Cambridge Structural Database" *Acta Crystallogr., Sect. B: Struct. Sci., Cryst. Eng. Mater.* **2016**, *72*, 171.

(18) (a) Hamaguchi, T.; Inoue, Y.; Ujimoto, K.; Ando, I. "Synthesis, crystal structure and electrochemistry of a ruthenium complex coordinated with an ambidentate 2-mercaptopyridinato N-oxide ligand" *Polyhedron* **2008**, *27*, 2031. (b) Hung, J.-T.; Kumaresan, S.; Lin, L.-C.; Wen, Y.-S.; Liu, L.-K.; Lu, K.-L.; Hwu, J. R. "Reactions of 1-Hydroxypyridine-2-thione with Triosmium Clusters. Preparation and Transformation of N-Oxide-Containing Osmium Complexes" *Organometallics* **1996**, *15*, 5605. (c) Yuan, Z.-D.; Zhou, F.-X.; Zhang, H.-P.; Yue, C.-Y. "catena-[tris(m2-Aqua)-penta-aqua-di-sodium bis(bis(pyridine-2-thiolate 1-oxide)-gold) dihydrate]" *Chin. J. Inorg. Chem.* **2013**, *29*, 1283. (d) Zhang, G. "Polymorphism in unusual one-dimensional coordination polymers based on cadmium (II) and 2-mercaptopyridine N-oxide" *Cryst. Eng. Comm.* **2013**, *15*, 6453.

(19) For other μ-S and μ-O bridging coordination modes, see (a) Wang, X.-J.; Gui, L.-C.; Shen, Z.-S.; Ni, Q.-L.; Zeng, J.-Q. "Catena-Poly[cadmium(II)-di-μ-N-oxo-pyridine-2-thiol-ato]" *Acta Crystallogr., Sect.E: Struct. Rep. Online* **2006**, *62*, m931. (b) Barnett, B. L.; Kretschmar, H. C.; Hartman, F. A. "Structural characterization of bis (N-oxopyridine-2-thionato) zinc (II)" *Inorg. Chem.* **1977**, *16*, 1834.

(20) Deterioration of samples was observed by NMR in ~1 week when stored in either the solid or solution state at room temperature. Deterioration was generally reduced, but not prevented, by storing samples in the dark.

(21) (a) Bohne, C.; Boch, R.; Scaiano, J. C. "Exploratory studies of the photochemistry of N-hydroxypyridine-2-thione esters. Generation of excited radicals by laser flash photolysis and in a conventional fluorescence spectrometer" *J. Org. Chem.* **1990**, *55*, 5414. (b) Aveline, B. M.; Kochevar, I. R.; Redmond, R. W. "Photochemistry of N-hydroxypyridine-2-thione derivatives: involvement of the 2-pyridylthiyl radical in the radical chain reaction mechanism" *J. Am. Chem. Soc.* **1995**, *117*, 9699. (c) Aveline, B. M.; Kochevar, I. R.; Redmond, R. W. "Photochemistry of the Nonspecific Hydroxyl Radical Generator, N-Hydroxypyridine-2(1H)-thione" *J. Am. Chem. Soc.* **1996**, *118*, 10113.

(22) (a) Nayagam, B. R. D.; Jebas, S. R.; Jeyakumar, H. J.; Schollmeyer, D. "2-(Benzylsulfanyl) pyridine N-oxide" *Acta Cryst. Sect. E* **2008***, 64*, o928. (b) Wang, H-H.; Zhang, C-Y.; Cui, Y.; Xie, Y-B. "2, 2′-[Ethane-1, 2-diylbis (sulfanediyl)] bis (pyridine N-oxide)" *Acta. Cryst. Sect. E*, **2009**, *65*, o3268. (c) Hartung, J.; Svoboda, I.; Fueß, H. "Balancing Conjugational Stabilization and Torsional Strain. The Solid-State Structure of a 2-Thio-alkyl-Substituted Pyridine N-Oxide" *Acta Crystallogr., Sect. C: Cryst. Struct. Commun.* **1996**, *52*, 2841. (d) Nayagam, B. R. D.; Jebas, S. R.; Devadasan, J. J.; Schollmeyer, D. "2-(2,3,5,6-Tetra-methyl-benzyl-sulfan-yl)pyridine N-oxide" *Acta Crystallogr. Sect. E: Struct. Rep. Online* **2008**, *64*, o1975. (e) Nayagam, B. R. D.; Jebas, S. R.; Jeyakumar, H. J.; Schollmeyer, D. "2-(Mesitylmethylsulfanyl)pyridine N-oxide monohydrate" *Acta Crystallogr. Sect. E: Struct. Rep. Online* **2008**, *64*, o1952. (f) Hartung, J.; Svoboda, I.; Fueß, H. "Crystal structure of S-(2-phenyl-4-penten-1-yl)-2-thiopyridine N-oxide, $C_{16}H_{17}NOS$" *Z. Kristallogr.-New Cryst. Struct.* **1998**, *213*, 333. (g) Zhang, C-Y.; Gao, Q.; Cui, Y.; Xie, Y-B. "2,2′-[o-Phenylenebis(methylene-thio)]bis-(pyridine N-oxide)" *Acta Crystallogr., Sect. E: Struct. Rep. Online* **2009**, *65*, o1482. (h) Nayagam, B. R. D.; Jebas, S. R.; Samuelraj, C. R.; Schollmeyer, D. "2,4,6-Tris(1-oxo-2-pyridylsulfanylmeth-yl)mesitylene methanol solvate" *Acta Crystallogr., Sect. E: Struct. Rep. Online* **2008**, *64*, o1036. (i) Nayagam, B. R. D.; Jebas, S. R.; Grace, P. S.; Schollmeyer, D. "Tetra-kis{2,4-bis-[(1-oxo-2-pyridyl)-sulfanyl-methyl]mesitylene} acetone hemisolvate 11.5-hydrate" *Acta Crystallogr., Sect. E* **2009**, *65*, o129. (j) Nayagam, B. R. D.; Jebas, S. R.; Grace, S.; Schollmeyer, D. "2,2′-[2,3,5,6-Tetra-methyl-phenyl-ene-bis-(methyl-ene-thio)]bis-(pyridine N-oxide)" *Acta Crystallogr., Sect. E*, **2008**, *64*, o409.

(23) Hartung, J.; Hiller, M.; Schwarz, M.; Svoboda, I.; Fueß, H. "Solid State and Solution Structures of O-Alkyl- and of O-Acyl Derivatives of 1-Hydroxypyridine-2(1H)-thione" *Liebigs Ann.* **1996**, 2091.

(24) Hartung, J.; Kneuer, R.; Schwarz, M.; Svoboda, I.; Fueß, H. "On the Selective O-Alkylation of Ambident Nucleophiles – The Synthesis of Thiohydroxamic Acid O-Esters by Phase-Transfer Reactions" *Eur. J. Org. Chem.* **1999**, *1*, 97.

(25) Unlike in the related OPO complexes which suffered from C/N disorder in their X-ray structures, all of the structures of OPTO complexes reported here consisted of a single isomer.

(26) Bond, A.; Jones, W. "1-Hydroxy-2 (1H)-pyridinethione" *Acta. Cryst.* **1999**, *C55*, 1536.

(27) Bondi, A. "van der Waals volumes and radii" *J. Phys. Chem.* **1964**, *68*, 441.

(28) The other C—C bond lengths in the ring, expected to be influenced by π-ED, are not affected to an appreciable extent.

(29) The upfield chemical shift of **2** relative to **1** is not unusual as the ^{29}Si NMR signal of $Me_3Si(OPh)$ and $Ph_3Si(OPh)$ in $CDCl_3$ appear at δ +19.3 ppm and -14.6 ppm respectively. For $Me_3Si(OPh)$, see Schraml, J. *Collect. of Czechoslov. Chem. Commun.* **1990**, *55*, 2033. $Ph_3Si(OPh)$ was prepared independently.

(30) Sandwich-type intermolecular π-stacking occurs in **3** between the pyridine rings of the chelated OPTO ligands (N1, C1-C5 ~3.4 Å) which may influence the chelate bonding characteristics. The observed π-stacking may also relate to the strikingly low solubility of **3** in $CDCl_3$ in comparison with **4** and **5** having larger aliphatic ligands.

(31) de Klerk-Engels, B.; Groen, J. H.; Vrieze, K.; Möckel, A.; Lindner, E.; Goubitz, K. "Synthesis of new (cyclopentadienyl)rutheniumphosphine complexes with hemilabile ether-phosphines. The X-ray structure of $(\eta^5\text{-}C_5H_5)RuCl(Ph_2PCH_2CH_2OCH_3)_2$" *Inorg. Chim. Acta* **1992**, *195*, 237.

(32) The ^{29}Si NMR signal shifted from δ −28.4 ppm at 22 °C to −26.8 ppm at 50 °C, and the ^{13}C NMR C=S signal shifted from 169.6 ppm at 22 °C to 170.4 ppm at 50 °C.

(33) By comparison, the ^{29}Si NMR chemical shifts in $CDCl_3$ of the parent dichlorosilanes, $(CH_2)_3SiCl_2$, $(CH_2)_4SiCl_2$, and $(CH_2)_5SiCl_2$, appear at 18.1, 44.8 and 28.1 ppm, respectively. See Daiss, J. O.; Burschka, C.; Mills, J. S.; Montana, J. G.; Showell, G. A.; Warneck, J. B. H.; Tacke, R. *Organometallics* **2006**, *25*, 1188.

(34) Brendler, E.; Wächtler, E.; Wagler, J. "Hypercoordinate silacycloalkanes: Step-by-step tuning of N→ Si Interactions" *Organometallics* **2009**, *28*, 5459.

(35) (a) Denmark, S. E.; Griedel, B. D.; Coe, D. M.; Schnute, M. E. "Chemistry of Enoxysilacyclobutanes: Highly Selective Uncatalyzed Aldol Additions" *J. Am. Chem. Soc.* **1994**, *116*, 7026. (b) Spiniello, M.; White, J. M. "Crystal Structures of Bis[(8'-(dimethylamino)naphth-1'-yl)dimethylsilyl] Ether and Bis[(8'-(dimethylamino)naphth-1'-yl)-1-silacyclobut-1-yl] Ether. Structural Evidence for the Enhanced Lewis Acidity of Silacyclobutane Derivatives" *Organometallics* **2000**, *19*, 1350.

(36) Compared with their parent dichlorosilanes, $(CH_2)_4SiCl_2$ and $(CH_2)_5SiCl_2$, the C-Si-C angles in **8** and **9** also contract (Δ = 5.3 and 7.4°, respectively) upon complexation of the OPTO ligands. In **7**-**9**, the O, S-positions orthogonal to the basal plane of the silacycloalkane rings subtend at angles of 165.03(3), 164.48(5), and 161.16(12)°, respectively, away from the silacycloalkane rings. See Wagler, J.; Gericke, R. "Molecular structures of various alkyldichlorosilanes in the solid state" *Dalton Trans.* **2017**, *46*, 8875.

(37) The difference between the ideal bond angle in T_d vs. O_h geometries and the C-Si-C angle in $(CH_2)_3SiCl_2$ and **7**, respectively, decreases from 27.0 to 12.6° upon chelation with the OPTO ligand. Additionally, the silacyclobutane rings in both $(CH_2)_3SiCl_2$ and **7** are puckered effectively to the same extent with dihedral angles between C11–Si–C13 and C11–C12–C13 planes of 19.6(2) and 19.4(2)°, respectively, and between Si–C11–C12 and Si–C13–C12 planes of 18.2(2)° and 18.9(3)°, respectively.

(38) The structure of **9** is ~90% square pyramidal along the trigonal bipyramidal→square pyramidal Berry-pseudorotation continuum. See Kost, D.; Kingston, V.; Gostevskii, B.; Ellern, A.; Stalke, D.; Walfort, B.; Kalikhman, I. "Donor-Stabilized Silyl Cations. 3. Ionic Dissociation of Hexacoordinate Silicon Complexes to Pentacoordinate Siliconium Salts Driven by Ion Solvation" *Organometallics* **2002**, *21*, 2293.

(39) The preparation of $Ph_2Si(OPTO)_2$ was also attempted by trans-silylation of 2 equiv. of **1** with Ph_2SiCl_2 in $CDCl_3$ and resulted in a mixture of Me_3SiCl, $Ph_2Si(OPTO)Cl$, unreacted **1**, and additional unidentified peaks presumably of $Ph_2Si(OPTO)_2$ by ^{13}C and ^{29}Si NMR spectroscopy. The precipitation of an intractable solid prevented further purification.

(40) The tendency for chloride ligands to occupy axial positions is typical of most 5-coordinate chlorosilanes. See Corriu, R. J. P.; Kpoton, A.; Poirier, M.; Royo, G.; de Saxcé, A.; Young, J. C. "Pentacoordinated silicon compounds. Intramolecular ring closure, site preferences of substituents and the stability of the resulting chelates" *J. Organomet. Chem.* **1990**, *395*, 1.

(41) Patyk, E.; Marciniak, J.; Tomkowiak, H.; Katrusiak, A.; Merz, K. "Isothermal and isochoric crystallization of highly hygroscopic pyridine N-oxide of aqueous solution" *Acta Cryst.* **2014**, *B70*, 487.

(42) Wasada, H.; Hirao, K. "Theoretical study of the reactions of pentacoordinated trigonal bipyramidal phosphorus compounds: PH_5, PF_5, PF_4H, PF_3H_2, PF_4CH_3, $PF_3(CH_3)_2$, $P(O_2C_2H_4)H_3$, $P(OC_3H_6)H_3$, and PO_5H_4" *J. Am. Chem. Soc.* **1992**, *114*, 16.

(43) Miessler, G. L.; Tarr, D. A. *Inorganic Chemistry, 4th ed.* Pearson Education: Upper Saddle River, NJ, 2011; p 61.

(44) The structure of $Et_2Si(QNO)Cl$ will be published elsewhere..

(45) Ma, C.; Zhang, J; Zhang, R. "Syntheses, characterization, and X-ray crystal structures of diorganotin(IV) derivatives of 2-pyridinethiolato-N-oxide" *Can. J. Chem.* **2003**, *81*, 1070.

(46) The increased extent of solvation of **18** is supported by its deviation in the correlation plot of the ^{13}C NMR C=S chemical shift with average C—S bond distance (Figure 6). The low field appearance of its C=S resonance (δ 163.3 ppm) indicates a greater extent of Si←S bond dissociation than would be expected from the solid-state structure (average $d_{C—S}$ = 1.727 Å).

(47) Deviations from this arrangement are observed in one of the monodentate ligands of **6** and **10** with dihedral angles of 65.04(8) and 40.0(2)°, respectively.

(48) Relative chelate strength was assessed on the basis of the average carbon-sulfur bond lengths in each complex.

(49) These spectral changes with temperature might also be predicted for an S_{ax}/S_{eq} isomerization process, but we favor the Si←S bond dissociation process on the following bases: (1) From its X-ray structure, compound **9** has effectively a square pyramidal geometry and therefore does not support the presence of S_{ax} and S_{eq} isomers. (2) Hexacoordinate silicon compounds **7** and **8** exhibit the same pattern of ^{13}C and ^{29}Si NMR shifts with temperature. (3) We have observed qualitatively that the ^{13}C and ^{29}Si NMR chemical shifts of complexes with weaker Si←S interactions in the solid state, such as in **9**, are more sensitive to changes in temperature. (4) In our work with related OPO complexes, the same pattern of ^{13}C and ^{29}Si NMR spectral changes was observed for the parallel Si←OC bond dissociation equilibrium.

(50) The ^{13}C VT-NMR spectra of **8** in toluene-d_8 are given in Figure S48. No ^{29}Si NMR peak for **7** could be observed above room temperature.

(51) In toluene-d_8, the ^{29}Si NMR peak shifted from δ -93.0 to -86.3 ppm from -80 to 20 °C, respectively. In $CDCl_3$, the ^{29}Si NMR peak shifted from δ -87.9 to -80.2 ppm from -60 to 20 °C, respectively.

(52) For **5**, δ = -29.6 ppm, toluene-d_8; δ = -28.4 ppm, $CDCl_3$. For **8**, δ = -86.3 ppm, toluene-d_8; δ = -80.2 ppm, $CDCl_3$. For **15**, δ = -30.9 ppm, toluene-d_8; δ = -27.8 ppm, $CDCl_3$. For **1**, δ = 36.7 ppm, toluene-d_8; δ = 39.8 ppm, $CDCl_3$.

(53) Hartung, J.; Svoboda, I.; Duarte, M. T. "Hydrogen bonding in 1-hydroxy-4 (1H)-pyridinethione" *Acta Cryst.* **1997**, *C53*, 1631.

(54) Upon addition of 10 equiv. of $CHCl_3$ to **9** in toluene-d_8, carbon resonances **a-e** shifted downfield by 0.21, 0.28, 0.19, 0.07, and 0.12 ppm, respectively.

(55) Transition-metal thione and thioamide complex chloroform solvates with $Cl_3CH\cdots S$ interactions result in only a modest lengthening, if any, of their M—S bonds. (a) Akaiwa, M.; Kanbara, T.; Fukumoto, H.; Yamamoto, T. "Luminescent palladium complexes containing thioamide-based SCS pincer ligands" *J. Organomet. Chem.* **2005**, *690*, 4192. (b) Nuss, G.; Saischek, G.; Harum, B. N.; Volpe, M.; Gatterer, K.; Belaj, F.; Mösch-Zanetti, N. C. "Novel pyridazine based scorpionate ligands in cobalt and nickel boratrane compounds" *Inorg. Chem.* **2011**, *50*, 1991.

(56) Wagler, J.; Brendler, E. *Z. Naturforsch.* **2007**, *62b*, 225.

(57) Upon addition of 175 equiv of $CHCl_3$ to **15** in toluene-d_8, carbons **a-e** shifted proportionally downfield (Δ(δ) = 0.65, 0.70, 0.50, 0.12, and 0.40 ppm, respectively) in comparison with **9** and suggests a similar phenomenon in both.

(58) (a) Kummer, D.; Halim, S. H. A.; Kuhs, W.; Mattern, G. "Beiträge zur Chemie der Halogensilanaddukte: XXIII. Über die ionisierung der SiCl-Bindung. Temperaturabhängige Ubergänge zwischen penta- und tetrakoordinierten SiCl-Verbindungen. Die Kristall- und Molekülstruktur von Chloro-dimethyl-(3,4,7,8-tetrahydro-*2H,6H*-pyrimido[1,2-*a*]pyrimidin-1-ylmethyl-C_1,N_9)-silicium" *J. Organomet. Chem.* **1993**, *446*, 51. (b) Kummer, D.; Chaudhry, S. C.; Seifert, J.; Deppisch, B.; Mattern, G. "Contributions to the chemistry of halosilane adducts: XIX. Temperature dependent equilibrium between pentacoordinate and ionic tetracoordinate structures of an organochlorosilane-nitrogen base adduct. Synthesis and structural investigations of (N·Si)-silicon-functional (1-(2-pyridone(2′-pyridyl)imine)methyl)silanes. The crystal and molecular structure of (N·Si)-chloro(1-(2-pyridone- (2′-pyridyl)imine)methyl)dimethylsilane, (N·Si)-(1-(2- pyridone(2′-pyridyl)imine)methyl)trichlorosilane and 1-methyl-2-(2′-pyridyl)aminopyridinium chloride" *J. Organomet. Chem.* **1990**, *382*, 345.

(59) (a) Gerdes, C.; Saak, W.; Haase, D.; Müller, T. "Dibenzosilanorbornadienyl cations and their fragmentation into silyliumylidenes" *J. Am. Chem. Soc.* **2013**, *135*, 10353. (b) Weiß, J.; Theis, B.; Metz, S.; Burschka, C.; Guerra, C. F.; Bickelhaupt, F. M.; Tacke, R. "Neutral Pentacoordinate Halogeno- and Pseudohalogenosilicon(IV) Complexes with a Tridentate Dianionic O,N,O or N,N,O Ligand: Synthesis and Structural Characterization in the Solid State and in Solution" *Eur. J. Inorg. Chem.* **2012**, *19*, 3216. (c) Nakamoto, M.; Fukawa, T.; Sekiguchi, A. "Silylium ion to silylium ion rearrangement caused by 1, 3-methyl migration" *Chem. Lett.* **2004**, *33*, 38. (d) Xie, Z.; Liston, D. J.; Jelinek, T.; Mitro, V.; Bau. R.; Reed. C. A. "A new weakly coordinating anion: approaching the silylium (silicenium) ion" *Chem. Commun.* **1993**, 384.

(60) Cooling **15** in neat CD_3CN from 40 to -45 °C resulted in decoalescence of the methyl resonances, unidirectional upfield shifting of the ^{13}C OPTO ligand resonances, and a small downfield shift (1.0 ppm) of the ^{29}Si resonance. Taken as an AB site exchange, the activation energy ($\Delta G^{\ddagger}$) was calculated to be 14 kcal/mol using the equations $k = 2\pi(\Delta\nu)/\sqrt{2}$ and $\Delta G^{\ddagger} = -RT(\ln k - \ln(k_b T/h))$.

(61) (a) James, B. D.; Magee, R. J.; Patalinghug, W. C.; Skelton, B. W.; White, A. H. "Five-coordinate triphenyltin(IV)-sulfur compounds. Crystal structures of the aminoethanethiol and 2-mercaptopyridine-N-oxide derivatives" *J. Organomet. Chem.* **1994**, *467*, 51. (b) Ng, S. W.; Wei, C.; Das, V. G. K.; Mak, T. C. W. "First example of polytopal dominance of square pyramidal geometry in organotin pentacoordination: crystal structure of tribenzyl(2-thiolatopyridine-N-oxide)tin(IV)" *J. Organomet. Chem.* **1987**, *326*, C61. (c) Ng, S. W.; Wei, C.; Das, V. G. K.; Mak, T. C. W. "Skew-trapezoidal bipyramidal diorganotin(IV) bischelates. Crystal structure of dimethylbis(2-pyridinethiolato-N-oxide)tin(IV)" *J. Organomet. Chem.* **1987**, *334*, 295. (d) Ma, C.; Zhang, J. "Syntheses and crystal structures of diorganotin(IV) bis(2-pyridinethiolato-N-oxide) complexes" *Appl. Organometal. Chem.* **2003**, *17*, 788. (e) Ng, S. W.; Wei, C.; Das, V. G. K.; Mak, T. C. W. "Crystal structure of tribenzyl(2-pyridinethiolato-N-oxide)tin(IV): a rare example of a square pyramidal organotin(IV) compound" *J. Organomet. Chem.* **1987**, *334*, 283.

(62) The structure of $(mesityl)_2Si(OPO)_2$ will be published elsewhere.

(63) *APEX3*; Bruker AXS: Madison, WI, 2015.

(64) Sheldrick, G. M. *SADABS*; "Comparison of silver and molybdenum microfocus X-ray sources for single-crystal structure determination" *J. Appl. Cryst.* **2015**, *48*, 3-10.

(65) *SAINT*; Bruker AXS: Madison, WI, 2013.

(66) *CrysAlisPro*; Rigaku Corporation: Oxford, UK, 1995-2022.

(67) Burla, M. C.; Caliandro, R.; Camalli, M.; Carrozzini, B.; Cascarano, G. L.; Giacovazzo, C.; Mallamo, M.; Mazzone, A.; Polidori, G.; Spagna, R. "SIR2011: a new package for crystal structure determination and refinement" *J. Appl. Cryst.* **2012**, *45*, 357.

(68) Sheldrick, G. M. "A Short History of SHELX" *Acta Cryst*. **2008**, A*64*, 112-122.

(69) Sheldrick, G. M. *SHELXT*; "Crystal structure refinement with SHELXL" *Acta. Cryst.* **2015**, A*71*, 3-8.

(70) Dolomanov, O. V.; Bourhis, L. J.; Gildea, R. J.; Howard, J. A. K.; Puschmann, H. "OLEX2: a complete structure solution, refinement and analysis program" *J. Appl. Cryst.* **2009**, *42*, 339-341.

(71) Sheldrick, G. M. *TWINABS*; University of Göttingen, Germany, 2012.